INFORMATION TO USERS

This manuscript has been reproduced from the microfilm master. UMI films the text directly from the original or copy submitted. Thus, some thesis and dissertation copies are in typewriter face, while others may be from any type of computer printer.

The quality of this reproduction is dependent upon the quality of the copy submitted. Broken or indistinct print, colored or poor quality illustrations and photographs, print bleedthrough, substandard margins, and improper alignment can adversely affect reproduction.

In the unlikely event that the author did not send UMI a complete manuscript and there are missing pages, these will be noted. Also, if unauthorized copyright material had to be removed, a note will indicate the deletion.

Oversize materials (e.g., maps, drawings, charts) are reproduced by sectioning the original, beginning at the upper left-hand corner and continuing from left to right in equal sections with small overlaps.

Photographs included in the original manuscript have been reproduced xerographically in this copy. Higher quality 6" x 9" black and white photographic prints are available for any photographs or illustrations appearing in this copy for an additional charge. Contact UMI directly to order.

ProQuest Information and Learning
300 North Zeeb Road, Ann Arbor, MI 48106-1346 USA
800-521-0600

Preparation of a Stable Double Emulsion; Study of the Factors Affecting the Stability Of the System (W1/O/W2)

by

MOUHCINE KANOUNI

A dissertation submitted to the Graduate Faculty in Chemistry in partial fulfillment of the requirements for the degree of Doctor of Philosophy, The City University of New York

2001

UMI Number: 3024805

Bell & Howell Information and Learning Company
300 North Zeeb Road
P.O. Box 1346
Ann Arbor, MI 48106-1346

This manuscript has been read and accepted for the Graduate Faculty in Chemistry in satisfaction of the dissertation requirements for the degree of Doctor of Philosophy.

07/20/2001
Date

Chair of Examining Committee

7/26/2001
Date

Executive Officer

David C. Locke
Professor Locke

Chas Maldarelli
Professor Maldarelli

D. Jon, Ph.D.

Supervisory Committee

The City University of New York

Abstract

PREPARATION OF A STABLE DOUBLE EMULSION STUDY OF THE FACTORS AFFECTING THE STABILITY OF THE SYSTEM (W1/O/W2)

by
Mouhcine Kanouni

Advisor: Professor Henri L. Rosano

The primary objective of the research was to prepare double emulsions of the type W1/O/W2 and investigate the factors affecting the mechanism of formation and the emulsions' stability respectively. A review of the literature indicates that stability of double emulsions requires a balance between Laplace and the osmotic pressure between W1 droplets in oil and between W1 droplets and the external aqueous phase W2. It was assumed a priori that the different interfacial films, W1/O and O/W2, were completely stable.

The study focused mainly on the formulation of two different systems: 1) the formulation of a stable W1/O/W2 emulsion using mineral oil with a concentration of over 12% of surfactant in the outer aqueous phase; 2) the formulation of a stable edible multiple emulsion using soybean oil. A stable emulsion (W1/O) is a critical first step to achieve before preparing a stable W1/O/W2 double emulsion. Consequently, we initially focused on the preparation of the primary emulsion, W1/O, and investigated the role of the W1/O film on the stability of the emulsion.

Among the different classes of primary surfactants (low Hydrophile-Lipophile Balance) that we tested, only cetyl dimethicone copolyol (Abil Em90), A-B-A block copolymer (Arlacel P135), and polyglycerol ester of ricinoleic acid (Grinstead PGR90) produced a stable W/O emulsion.

The mechanical and electrical surface properties of these surfactants were also investigated using a monolayer technique. These three surfactants showed the following similar surface properties: 1) stable compressible and reversibly expandable monolayer 2) irreversible adsorption at the interface 3) high elasticity and 4) high surface potential. The high values obtained for film elasticity give the interfacial film strong resiliency during stress. According to the high surface potential observed, the surfactant molecules appear to lie flat at the oil/water interface. In the case of polyglycerol ester of ricinoleic acid, the –OH groups on the fatty acid chains seem to serve as anchors at the O/W interface and are responsible for the high surface potential.

We also found that the presence of a thickener is necessary in the outer aqueous phase in order to reach a viscosity ratio of about 1 with W1/O. This allows the dispersion of the viscous primary emulsion into the W2 aqueous phase. The presence of the thickener also prevents phase separation due to its thixotropic property. However, the thickener must be compatible with the surfactants. Finally, another factor that needs to be considered is the interaction between the low and high HLB emulsifiers. In order to prevent destabilization of

the films, the addition of the high HLB surfactant in W2 should not interact by displacement with the low HLB surfactant at the O/W_2 interface.

Acknowledgments

بِسْمِ ٱللَّهِ ٱلرَّحْمَٰنِ ٱلرَّحِيمِ

My first thank obviously goes to Professor Rosano who is more than a mentor to his graduate students. Professor Rosano has this quality of enhancing what is best within his graduate students and also to guide them with an exceptional sense of confidence. Dr. Rosano, as I heard once, represents the epitome of the polyvalent scientist who is capable of bringing together the expertise of scientists of different backgrounds and with his remarkable knowledge in the field of surface chemistry, solves whatever problem is given.

At this point, I would also like to thank my father for whom this PhD represents a lot more that what we can think of. My father has always been the "engine". In fact, I should thank my all family for their support, Thank you ALL.

I feel the deepest gratitude for the financial support provided by Unilever, Edgewater-NJ and Unilever, Somerset-NJ. I would particularly like to thank Michael Aronson, Thomas Grossberger and Guy Levi.

I would like to thank my friends: Christopher C. and Marie A. for her editorial help; Shaheed M. and Betty K. for their exceptional support and all my friends at Ciba (the list will be here to long to type).

I would like to thank various members of the faculty of the City University of New-York for their support during those years: Professor Koeppl (Executive Officer of the Doctoral Program in Chemistry), Professor Stanley Radel (Chairman of the Chemistry Dept. at City College of New York.

TABLE OF CONTENTS

LIST OF TABLES

LIST OF FIGURES

PREPARATION OF A STABLE DOUBLE EMULSION, STUDY OF THE FACTORS AFFECTING THE STABILITY OF THE SYSTEM (W1/O/W2)

1. Introduction

1 INTRODUCTION / OBJECTIVES

1.1 Uses and Application / Objectives

Currently, multiple emulsions are infrequently used. Their potential applications are, however, numerous, and the studies of these systems are now an active field of research [1,2,3,4,5], especially in such product areas as drug-delivery systems, cosmetics, and foods. Water/Oil/Water (W1/O/W2) emulsions allow the encapsulation of active molecules in the internal aqueous phase, thus allowing one to mask taste or smell; protect against oxidation, light, or enzymatic degradation; or to provide controlled liberation of the active ingredients under the effect of dilution, shearing, or agitation. Examples of research of multiple emulsions containing insulin in the internal aqueous phase have been tested orally on diabetic rats [6]. In cosmetic or food-chemistry applications, multiple emulsions have the potential to allow mayonnaise, sauce, or hand-cream formulations to yield a more agreeable aqueous feel than the usually oily texture. The first objective targeted was to be able to formulate a stable double emulsion W1/O/W2 with a concentration of 15% of surfactant in the outside aqueous phase W2. All previous formulations described in the literature contain at most 2 to 4% of surfactant in W2 [5]. The target of 15% was chosen to meet the typical cosmetic industrial standard for surfactant levels. The second objective of the research was to formulate a double emulsion using soybean oil as the oil

phase. In most of the previous studies[1,2,3], paraffin or mineral oil was used. In the rare instances when soybean oil was employed, difficulty arose in stabilizing the emulsion[8]. We believe the difficulty in obtaining a stable double emulsion with soybean oil was due to its higher solubility in water than the other type of oil.

1.2 Definitions and Characteristics

1.2.1 General definition:

In emulsions, one phase is dispersed throughout the second phase as "globules". An emulsion consists, then, of a dispersed phase (internal phase, discontinuous phase), a dispersion medium (external phase, continuous phase) and a third component known as an emulsifying agent. There are different types of emulsifying agents as will be discussed later. The diameter of the dispersed phase globules is generally in the range of about 0.1 to 10μ, though some as small as 0.01μ and as large as 100μ are not uncommon. Emulsions are used when two immiscible liquids must be dispensed in the same preparation for some designated reason. Ordinarily, this means there is a polar and a nonpolar component, each of which is a liquid. When the dispersed phase is nonpolar (oil) and the external phase is polar (water), the emulsion is known as an oil-in-water emulsion. When the dispersed phase is water and the dispersion medium is oil, the emulsion is of the water-in-oil

kind. Ordinarily, but not always, emulsions for internal use are of the oil-in-water type, and emulsions for external use are of either water or oil.

1.2.2 Water-in-oil emulsion (W/O)

Water-in-oil emulsions are insoluble in water, not water-washable, will absorb water, are occlusive, and may be "greasy".

1.2.3 Oil-in-water emulsions (O/W)

Oil-in-water emulsions are miscible with water, are water washable, will absorb water, are nonocclusive, and are nongreasy.

1.3 Emulsion Stability

1.3.1 Summary of previous studies on the stabilization of emulsion

The stability and formation of multiple emulsions have been intensively studied recently [7,8,9]. As a stability criterion for double emulsion, it was found necessary to balance the osmotic pressure with the Laplace pressure [10] in order to avoid Ostwald ripening [11]. In addition, the physical-chemical properties of the surfactants at the interface O/W and the interaction of the surfactants dissolved in the aqueous phase were found to

play a major role in the stability of the emulsions. Thus, Rosano et al. [10] and Ficheux et al.[12] found that the increase of concentration of a surfactant, such as sodium dodecyl sulfate (SDS), in W2, destabilizes the multiple emulsion. This paper is a continuation of our investigation of the preparation and stability of W1/O/W2 emulsions[13]. Our previous article developed both theoretical and experimental approaches to the stability of $W_1/O/W_2$ multiple emulsions. The theoretical approach emphasized the role of Ostwald ripening in countering stability in W/O emulsions. It also discussed the addition of an oil-insoluble solute (NaCl in our case) to the inner water phase of the system in order to prevent this "ripening" mechanism. The approach assumed complete stability of the $W_1/O/W_2$ interfacial films and no diffusion of salt from W_1 to W_2. The oil-insoluble solute (NaCl) was shown to stabilize both the first W_1/O emulsion and the inner water droplets at the O/W_2 interface. Experimentally, the presence of an electrolyte in W_1 was necessary for stability to the multiple emulsion.

Three possible factors seemed to influence the stability of $W_1/O/W_2$:

(1) Laplace and osmotic effects between the water droplets in the W_1/O emulsion and the two aqueous phases, W_1 and W_2.

(2) Interactions between the low and high Hydrophile-Lipophile Balance (HLB) emulsifiers at the O/W_2 interface.

(3) Polymeric thickener-hydrophilic emulsifier's interactions in the outer phase (W_2).

Based on these theoretical considerations, our approach to preparing stable W1/O/W2 emulsions emphasized the choice of surfactants and polymeric thickeners as well as the proper amount of salt added to W1. The research undertaken seeks to clarify certain aspects of the interactions enumerated above (between low- and high HLB emulsifiers and between polymeric thickeners and hydrophilic emulsifiers) that were previously not explained. The objective of this study was also to analyze the role of the interfacial film formed by the low HLB surfactant. This paper investigates the primary interface W/O and studies the properties of the monolayer of a) cetyl dimethicone copolyol b)the polyglycerol ester of ricinoleic acid, and c) PEG-polyhydroxystearate copolymers.

1.4 Some other factors affecting the stability

It is well known but still necessary to be emphasized that emulsion stability can be enhanced by:

* decreasing the globule size of the internal phase
* obtaining an optimum ratio of oil to water
* increasing the viscosity of the emulsion.

If the globule size is reduced to less than 5 microns, the stability and dispersion of the emulsion will increase. This can be accomplished with the shearing action of a Turrax and a homogenizer. The optimum phase volume ratio generally is obtained when the internal phase is about 40-60% of the total quantity of the product. As the percentage of the internal phase

increases, the viscosity of the product also increases. Also, enhancement of viscosity of the external phase will tend to enhance the stability of the emulsion[14]. This is accomplished by the addition of a substance which is soluble in or miscible with the external phase of the emulsion. For o/w emulsions, hydrocolloids can be used. For w/o emulsions, waxes and viscous oils as well as fatty alcohols and fatty acids can be used. Of obvious concern in the preparation of emulsions is their physical stability. This is characterized by an absence of creaming and coalescence and the maintenance of the original appearance, odor, color and other physical properties.

1.5 Composition

Generally, emulsions contain three components: a lipid phase, an aqueous phase and the emulsifier. Of these, the compounding pharmacist generally has greatest flexibility in the choice of the emulsifier. Emulsifiers that can be used are shown in Table 1.

1.6 Determination of Type of Emulsions

It is important to know whether an emulsion is o/w or w/o in the event additional ingredients must be added. The type of emulsion can be

determined by some simple tests, including the drop dilution test, dye solubility test, electrical conductivity test, and the filter paper test. The drop dilution test is based on the principle that an emulsion is miscible with its external phase and the test is simply performed by dropping a small quantity of the emulsion onto a surface of water. If the drop is miscible with the water, it will spread, indicating that water is the external phase (an o/w emulsion). The dye solubility test is based on the principle that a dye disperses uniformly throughout an emulsion if it is soluble in the external phase and the dye test is conducted by adding a small quantity of a water soluble dye (powder or solution) to the emulsion. If it diffuses uniformly throughout the emulsion, water is the external phase (an o/w emulsion). The electrical conductivity test is based on the principle that water conducts an electric current, while oils do not. Generally, o/w emulsions have a tendency to conduct electricity better than w/o emulsions, if the required equipment is available. The filter paper test involves putting a drop of emulsion onto a clean piece of filter paper. If the drop spreads rapidly into the filter paper, it is an o/w emulsion as water (the external phase) tends to spread more rapidly throughout the filter paper than does oil.

1.7 Emulsifying Agents

The purpose of an emulsifying agent is to minimize the tendency of the globules to coalesce, or join together to form larger globules, with eventual

separation of the two liquids. The stability of an emulsion is dependent upon the properties of the emulsifier and the film it forms at the interface between the two phases. The film at the interface must be both tough and elastic and should be rapidly formed during the preparation, or emulsification, process. There are three different general methods whereby emulsifying agents aid in the formation of emulsions. These include:

1. Reduction of interfacial tension
2. Formation of a rigid interfacial film
3. Formation of an electrical double layer

If the emulsifier concentration is sufficiently high, a rigid film can be formed between the immiscible phases which can act as a mechanical barrier to coalescence of the globules. An electrical double layer results in repulsive electrical forces between approaching droplets to minimize coalescence.

Emulsifying agents can be divided into three different categories:

1.7.1 Surface-active agents

1.7.1.1 Hydrophilic colloids

Finely divided solid particles

Surface-active agents are adsorbed at oil:water interfaces to form monomolecular films, resulting in a decrease in interfacial tension.

Hydrophilic colloids form multi-molecular films about the dispersed particles. Finely divided solid particles are adsorbed at the interface between the two liquid phases of the globules and form a film of particles around the dispersed globules. Common to each of these three categories is the formation of a "film".

1.7.1.2 HLB

The HLB (Hydrophile-Lipophile Balance) system is used for describing the characteristics of a surface-active agent. It consists of an arbitrary scale to which HLB values are experimentally determined and assigned. If the HLB value is low, there are a small number of hydrophilic groups on the surfactant and it is more lipophilic (oil soluble) than hydrophilic (water soluble). For example, Span 80 has an HLB value of 4.3, from Table 2, and is oil soluble. If the HLB value is high, there is a large number of hydrophilic groups on the surfactant and it is more hydrophilic (water soluble) than oil soluble. For example, Tween 20 has an HLB value of 16.7 and is water soluble. Some general applications of materials with various HLB values are as follows:

Low 1-3 Antifoaming agents

3-6 Emulsifying agents (w/o emulsions)

7-9 Wetting agents

High 8-18 Emulsifying agents (o/w emulsions)

13-16 Detergents

16-18 *Solubilizing agents*

1.7.2 Wetting agents

Wetting agents are surfactants with HLB values of 7 to 9. Wetting agents aid in attaining intimate contact between solid particles and liquids. Emulsifying agents are surfactants with HLB values of 3 to 6 or 8 to 18. Emulsifying agents reduce interfacial tension between oil and water resulting in minimizing surface energy through the formation of globules. Detergents are surfactants with HLB values of 13 to 16. Detergents will reduce the surface tension and aid in wetting the surface and the dirt. The soil will be emulsified, foaming may occur, and the dirt will wash away. Solubilizing agents have HLB values of 16 to 18.

An HLB of 10 or greater is primarily hydrophilic and less than 10 would be lipophilic. Spans have HLB values ranging from 1.8 to 8.6, indicative of oil-soluble or oil-dispersible molecules. Consequently, the oil phase will predominate and the emulsion formed will be water-in-oil. Tweens have HLB values between 9.6 to 16.7, characteristic of water-soluble or water-dispersible molecules. Therefore, the water phase will predominate and oil-in-water emulsions will be formed.

1.7.3 Blending of Surfactants

Often a blend of emulsifiers produces a more stable emulsion than the use of a single emulsifier with the correct, calculated HLB. Since the HLB numbers are additive, the HLB value of a blend can be calculated.

For example, if 20 mL of an HLB of 9.65 are required, then two surfactants (with HLB values of 8.6 and 12.8) can be blended in a 3:1 ratio. The following quantities of each will be required:

3/4 x 8.6 = 6.45 (15 mL)

1/4 x 12.8 = 3.20 (5 mL)

TOTAL HLB = 9.65 (20 mL)

1.8 Preservation of Emulsions

Emulsions will support microbiological growth. Contamination of the products can occur during the preparation of the emulsion as well as during its use. To minimize contamination, the work area and equipment should be clean and every attempt made to produce a "clean" product. However, if the product is to be stored for any length of time, consideration must be given to the addition of a preservative. A preservative must be nontoxic, stable,

compatible, inexpensive, and have an acceptable taste, odor and color. It should also be effective against a wide variety of bacteria, fungi and yeasts. Preservatives may partition into the oil phase and lose their effectiveness. Bacterial growth normally will occur in the aqueous phase. Consequently, the preservative should be concentrated in the aqueous phase. Additionally, since the un-ionized form of the preservative will be more effective against bacteria, the majority of the preservative should be present in the non-ionized state. The preservative must neither be bound nor adsorbed to any agent in the emulsion or the container in order to be effective. In summary, only the preservative in the aqueous phase in the free, unbound, unadsorbed, un-ionized state will be effective in emulsions. The parabens (methylparaben, propylparaben, butyl-paraben) are among the most satisfactory preservatives for emulsions.

1.8.1 Antioxidants for Emulsions

Oils and fats are subject to rancidification resulting in a product exhibiting an unpleasant odor, appearance and taste. In order to minimize this, antioxidants can be added to the preparation. Example antioxidants are listed in Table 3.

1.9 General Comments on Emulsions

The viscosity of an emulsion generally increases upon aging.

The greater the volume of the internal phase, the greater the apparent viscosity.

There is a linear relationship between emulsion viscosity and the viscosity of the continuous phase.

It has been said that, under a given set of conditions, an oil-in-water emulsion is more easily produced with glass equipment and a water-in-oil emulsion is more easily produced with water-repellent plastic equipment. This could be related to the "wettability" of the external phase in contact with the surface of the equipment.

PREPARATION OF A STABLE DOUBLE EMULSION, STUDY OF THE FACTORS AFFECTING THE STABILITY OF THE SYSTEM (W1/O/W2)

2. Methods

2 Materials and method

2.1 Materials

In most of the previous studies, paraffin or mineral oil was used. In the rare instances when soy bean oil was employed, difficulty arose in stabilizing the emulsion [14]. We believe the difficulty in obtaining a stable double emulsion with soybean oil was due to its higher solubility in water than the other type of oil. In our current study, we have experimented with two types of oil: mineral oil and soybean oil.

The oil phase was light mineral oil (LP) (Fischer Scientific, Fair Lawn, NJ), hexadecane (Sigma, Saint Louis, MO), or octyl palmitate (Goldschmidt Chemical Corp., Hopewell, VA) and soybean oil (Bestfoods North America).

The lipophilic polymeric emulsifiers intensively studied and used for the preparation of the W_1/O emulsions are:

- Abil EM 90®, a cetyl dimethicone copolyol (Goldschmidt Chemical Corp., Hopewell, VA) with a molecular weight of 14,000 [15,16,17].
- Arlacel P135®, a PEG-30 Dipolyhydroxystearate [18], block copolymer with a molecular weight of 5000 (ICI Surfactants, Wilmington, DE)
- Polyglycerol ester of ricinoleic, Grinstead PGR90® (Danisco Ingr., Inc., New Century, Kansas).

The hydrophilic emulsifier used was either sodium lauryl ether sulfate (SLES) ethoxylated (STEOL CS-330®, Stepan Company, Northfield, IL 60093; 28.5% active) or sodium dodecyl sulfate (SDS) (Aldrich Chemical Company, Milwaukee, WI). We also used cocamidopropylbetaine (Betaine) (Tego Betaine F®, Goldschmidt Chemical Corp., Hopewell, VA; 30% active, 5% NaCl).

The polymeric thickeners tested were xanthan gum (XG) and guar gum (GG) (Colony Industries Inc., Holtsville, NY), carbopol 941® (CP) (BF Goodrich, Cleveland, OH), and hydroxyethylcellulose (HEC) (Aqualon Division, Hercules Inc., Wilmington, DE).

2.2 Method

Using techniques and materials similar to those described earlier[10], we prepared W1/O/W2 emulsions and investigated their stability visually and through video-microscopy. (Table 4, 5 and 6 show the standard formulations, modified by the results of the current study). We first studied the surface monolayer properties of Abil, both to enable the calculation of the minimum amount needed to prepare W1 and to clarify the high-HLB/low-HLB interactions. After calculating the minimum amount of Abil needed to prepare W1, we considered the optimum amount of salt needed to stabilize both the initial emulsion and the final W1/O/W2 system. We then selected the appropriate thixotropic water-soluble polymer. Guided by results from

our earlier work, we prepared emulsions in the following multi-step method: a W/O emulsion is obtained by emulsifying an aqueous phase in an oil phase containing a low HLB emulsifier (Table 5), using an Ultra-Turrax mixer at 9500 rpm for 10 minutes. Next the emulsion is added drop-wise to the aqueous phase (W2) containing a high HLB emulsifier and a thickener (Table 5 and 6). The second step is realized with reduced mechanical work (600 rpm mechanical stirrer for 5 minutes for the addition of W1/O to W2 and then 1000 rpm mechanical stirrer for 10 minutes). When this operation is completed, a second high HLB emulsifying surfactant may be added slowly with minimum mechanical work (400-rpm mechanical stirrer).

2.3 **Mechanical equipment**

The dispersions of water in oil or oil in water were made either with an Ultra-Turrax mixer (model Antrieb T25, Janke and Kunkel, Staufen, Germany) or with a mechanical stirrer.

2.4 **Evaluation techniques**

2.4.1 Microscopic and visual observations

Samples of all emulsions prepared were stored at room temperature for visual observation (i. e., checking for physical separation of the emulsion into two phases). The microscopic structure was tracked by video-microscopy (Axiovert 135 inverted microscope, Carl Zeiss Inc., Germany). The samples were prepared with caution to prevent deformation of the droplets and even breakdown of the multiple emulsion due to the stress produced by the cover slide.

2.4.2 Rheological measurements

The rheological analyses were performed at room temperature using a synchro-lectric model LVT Brookfield viscometer.

PREPARATION OF A STABLE DOUBLE EMULSION, STUDY OF THE FACTORS AFFECTING THE STABILITY OF THE SYSTEM (W1/O/W2)

3. Experimental

3 EXPERIMENTAL

The force-area (ΔA) and surface potential-area ($\Delta V/\Delta A$) characteristics of the low HLB surfactants at the air-water interface have been extensively investigated. The experimental apparatus for measuring surface pressures and potentials is shown in Figure 1. All experiments were conducted within a Faraday box.

The surfactant solution in *n*-hexane was deposited onto the aqueous surface with an Alga micrometer syringe (Burroughs Wellcome and Co., Tuckahoe, NY.).

The substrate and film were retained in a fused silica trough (31.2 x 13.6 x 2.5 cm) of 1.5-liter capacity. The surface was cleaned by dusting calcinated talcum powder onto it and removing it with the aid of a hollow glass tip connected to an aspirator.

3.1 Surface isotherms

3.1.1 Surface pressures

Surface pressures were determined from the surface tension measurements, which were made by suspending a sandblasted platinum

blade from a transducer-amplifier (Model 311A, The Sanborn Co, Waltham , Mass.). The transducer output was recorded continuously on a recorder (Mocon, type DB/40, Kipp & Zonon, Holland).

3.1.2 Surface potentials

Surface potentials were measured with an air-ionizing electrode[19] (a radium-226 source, U.S. Radium Corp., Morristown, NJ) placed 1 to 2 mm. above the surface of the liquid substrate, and connected to a precision potentiometer (Model 2730, Honeywell, Denver Division), a high-input resistance electrometer (Model 610B, Keithley Instruments Inc., Cleveland, Ohio) and a trough electrode (Ag/ AgCl or calomel) dipped into the bulk of the aqueous substrate. The radioactive electrode was connected to the input terminal of the electrometer with Amphenol low noise graphitized shielded cable and connectors.

The e.m.f of the cell, composed of the radioactive electrode, trough electrode, potentiometer, and electrometer, all connected in series, was measured immediately after cleaning the surface of the aqueous substrate (Vo), and compared with the e.m.f after spreading a film on the surface (v). The difference between the two e.m.f's (V - Vo) is the surface potential. The potentiometer opposed a convenient fraction of the cell e.m.f, and the electrometer output was recorded continuously on a recorder. An automatic barrier drive with variable speed control permitted determination of an

optimum compression rate and reproducible ΔA and ΔV-A isotherms. The continuous reduction of the surface area results in a measured surface pressure for stable films, which are considerably above their "equilibrium spreading pressures" (ESP), but still below their "monolayer stability limit" (MSL), which is defined [20] as the maximum pressure attainable in the film without collapse.

3.2 Particle Size Determination

Particle size analysis of formulation of water/oil emulsions was performed using a Brookhaven Instrument BI 90 plus (light scattering). In this analysis, the diluent (soy bean oil) was filtered with a 0.1micro m PTFE syringe filter before adding the concentrate. The soybean oil that was supplied appeared to be free of debris but upon filtration, the oil was visibly cleaner and crystal clear. Approximately 10 ml of the soybean oil was filtered into a 20mL scintillation vial. One drop of the W1/O emulsion was placed in the plain oil and agitated manually and using a mini-vortex. The diluted sample was agitated until a uniformity of color and turbidity was reached. About 3.5mL was decanted into a square plastic sampling cuvette and the cuvette was capped and placed in the 90 plus particle size analyzer. The analysis of each sample consisted of five to three minutes runs for a total run time of fifteen minutes

3.3 Pendant drop method to measure dynamic interfacial tension

Rennan P. et al[21] arrangement was used to measure the equilibrium and dynamic tensions by the static pendant drop and follows that of Lin et al.[22]. White light generated from a tungsten bulb is collimated and reduced in intensity by a series of pinholes, lenses and filters. The collimated beam is passed through a transparent quartz cell (2.5x4x4 cm) which is thermostated (23 ± 0.5°C). A drop of oil is formed at the tip of an inverted stainless steel, flat tipped capillary using a syringe. The growth of the drop is stopped when the diameter of the droplet reaches 2 to 3 mm. The formation of the drop does not require more than a second. Parallel light passing over the drop creates a silhouette of the pendant drop which is then imaged onto a CDD array video camera (Sony XC-77) using an objective lens. A PC operated Scion LG-3 frame broad, using N.I.H software, digitizes and saves as many as 30 images per second to RAM. A timer (FOR.A, Japan) records the time directly onto the video frames allowing the captured frames to be sequenced accurately. Distances on the video images are calibrated using a tungsten sphere of known diameter (1.5876 mm). Laplace equations describing the bubble shape are numerically integrated. Their solutions are then fitted to an edge profile obtained by image digitization by adjusting the surface tension[23]. The surface tension of pure water using this technique is 72.3 mN/m at 23 ± 0.5°C.

PREPARATION OF A STABLE DOUBLE EMULSION, STUDY OF THE FACTORS AFFECTING THE STABILITY OF THE SYSTEM (W1/O/W2)

4. Results

4 Results and Discussion

Among the different classes of primary surfactants (low HLB) tested (Table 4), we found three (figure 2) that allowed us to prepare a stable W1/O/W2 emulsion - over a 1 month period, at room temperature:

* Cetyl dimethicone copolyol (Abil Em90®)
* A-B-A block copolymer (Arlacel P135®)
* Polyglycerol ester of ricinoleic acid (Grinstead PGR90®)

We investigated the primary interface W/O and studied the properties of the monolayer of cetyl dimethicone copolyol; the polyglycerol ester of ricinoleic acid; and PEG- polyhydroxystearate copolymers.

4.1 Monolayer experiments- Study of the Primary Interface

A Langmuir trough was used to measure surface pressure versus surface area. Figure 3 and 4 represent the compression-decompression isotherms, surface pressure, of the cetyl dimethicone copolyol and the polyglycerol ester of ricinoleic, respectively, dissolved in n-hexane and spread on a 1% NaCl foamed solution (to insure that no extraneous surface-active

substances were present). The two monolayers exhibit similar properties: (a) surface pressure as high as 35 mN/m and (b) perfectly reversible compression-decompression isotherms. This latter property (b) supports the argument that when these basically insoluble substances are adsorbed at the oil/water interface, they can be subjected to mechanical constraints without structural damage.

In Figure 4, an inflection point in the compression of PGR90, situated at around 300 $Å^2$/molecule, is observed early, as revealed by a maximum in the apparent elasticity (figure 6). This point seems to indicate a maximal condensation of the two-dimensional phase and gives the limiting area occupied by an agglomeration of molecules. At higher surface coverage, a pseudo plateau is noticeable and suggests the appearance of a three-dimensional phase involving the expulsion of PRG90.

In figure 6, we determined the elasticity at the 3 different segments of the isotherms of the polyglycerol ester of ricinoleic. It is noticeable that the elasticity increases when the pseudo-plateau is reached and decreases after further compression. These changes of the elasticity are also reflected in the surface potential isotherm (figure 5). It is important to note, from figure 6, the extremely high values found for the elasticity (56.1, 174, 123) as compared to the elasticity values (6.2, 15.0, 24.3) found by Rosano et al.[24], for a DPPC film. Rosano and al. concluded on the importance of increased film elasticity on the stability of an emulsion. Consequently, in our study, the

high values obtained for film elasticity gives the film strong resiliency during stresses so it does not break and allows for a stable emulsion.

In figure 5 and 7, which represent the surface potential of PGR90 and PEG- polyhydroxystearate copolymer respectively, it is noteworthy to report the initial high surface potential (about 320 mV), indicating, that even before compression of the film, the strong orientation of the surfactant molecules at the interface. This result is comparable to those obtained by Habif et al[25]. Thus the hydroxy group directed into the water phase leads to a high surface potential. We are assuming that the expulsion of the PGR90, involving mostly the hydroxy group in the molecule, occurred toward the aqueous subphase, because of the high affinity of this functionality for water. This, then explains the increased potential observed in figure 5 at the same compression area. We believe that this process may be initiated before reaching the plateau and, more precisely, after a close-packed film is formed (increase of ΔA and ΔV). Later during the compression of the film, the observed decrease of the surface potential correlates with the increased surface pressure and, further, suggests the expulsion of the hydroxyl function to the opposite of the water subphase (repulsion of the function).

4.2 Investigation on Polyglycerol Ester of Ricinoleic Acid

Furthermore, in our search to identify PGR90, according to the description and properties of PGR90 received from the manufacturer of the product, the polyglycerol moiety shall be composed of not less than 75% of di-, tri- and tetraglycerols and shall contain not more than 10% of polyglycerols equal to or higher than heptaglycerol. Using this information, we calculated the GMW of the various esters. Also the manufacturer lists the iodine value of PGR90 to be 72-103, which represents the number of grams of iodine absorbed per 100g of a substance. Assuming I_2 (254 grams per one double bond), we calculated the GMW and iodine value of the various esters:

a) Oligomer: Di-glycerol

Ester Mw di-glycerol: 166g/mol	Mw (g/mol)	Iodine Value
1 acid + di-glycerol	438.5	48.85
2 acids + di-glycerol	715	71.35
3 acids + di-glycerol	992.5	76.8
4 acids + di-glycerol	1273	79.81

b) Oligomer: Tri-glycerol

Ester Mw tri-glycerol: 240g/mol	Mw (g/mol)	Iodine value
1 acid + tri-glycerol	520	48.8
2 acids + tri-glycerol	801	63.4
3 acids + tri-glycerol	1081	70.4
4 acids + tri-glycerol	1362	74.6
5 acids+ tri-glycerol	1642	77.3

c) Oligomer: Tetra-glycerol

Ester Mw tetra-glycerol: 314	Mw (g/mol)	Iodine value
1 acid + tetra-glycerol	613.5	41.4
2 acids + tetra-glycerol	875.3	56.52
3 acids + tetra-glycerol	1361.8	74.5
4 acids + tetra-glycerol	1467	86.5
5 acids + tetra-glycerol	1751.5	

From the previous tables, we can conclude that the Polyglycerol is highly esterified (at least 4 acids per glycerol, probably 5). The excess in the iodine value suggests a mixture of triglycerol and tetraglycerol oligomers, which is very common in the oligomerization process of glycerol. Assuming a GMW

of 1400, the area/molecule of an monolayer of PGR90 spread on water has been calculated.

The linear triglycerol has the following formula:

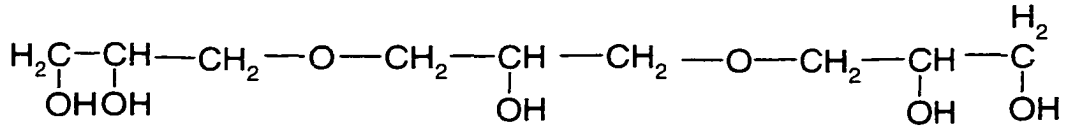

Assuming 1.5 Å between C-C, the molecule has a length of 15 Å. Ricinoleic acid (18carbon- cis) has a linear length of around 27 Å. The maximum surface area occupied by the polyglycerol ester would be 810 $Å^2$ per molecule. The surface isotherm (figure 5) shows that the surface pressure starts to increase below 400 Å which once again could indicate that although the molecules are still flat at the interface, at least two molecules must mesh and molecular repulsion starts.

4.3 *Interactions between the low and high HLB emulsifiers at the O/W_2 interface*

In Figure 3 we show a film of Abil EM90® produced a stable and reproducible compression surface isotherm at 22°C. Due to the great flexibility of the silicone backbone, the cetyl dimethicone copolyol chains can be compressed without any breakdown of the film. We did not reach the collapse pressure. The compression isotherm (Figure 8) of a duplex film [26] of Abil EM90®/Hexadecane does not show any interaction between the two

layers of the film. In Figure 9, after a film of Abil is spread and then compressed at 3 mN/m, 3mg of Betaine is injected under the film; after 30 minutes 3mg of SLES is injected. Throughout the experiment, the surface pressure is recorded as a function of time, showing a marked increase with each injection. The SLES is observed to penetrate into the film of Betaine adsorbed into the cetyl dimethicone copolyol film.

In a parallel experiment, the SLES is injected first and the Betaine 25 minutes later. This time, the surface pressure increases even more sharply for the SLES injection, but the Betaine produces no change in surface pressure. Calculating the slope at the beginning of the film penetration revealed that SLES penetrated into the Cetyl dimethicone film 2.7 times faster than Betaine. The absence of a second increase in slope indicates that Betaine does not penetrate into a Abil-SLES mixed monolayer.

As SLES penetrates more rapidly than Betaine, under the same conditions, it is obvious that the role played by the amount of mechanical work applied to the system is crucial. The results obtained with the mixed films Abil/SLES and Abil/Betaine suggest an explanation for the different paths followed by multiple emulsions prepared with Betaine as hydrophilic surfactant and those prepared with SLES. In the first case, the multiple structure remains after the addition of SLES. But we have seen that the penetration by SLES of an Abil film with a previous adsorption of Betaine is reduced. In the case of the multiple emulsions, this could explain the

decrease in size of the oil droplet during addition of SLES without over-emulsification of the first W_1/O (provided the amount of mechanical work is not too large). Since SLES is highly surface active at the air/Abil/water interface, and its adsorption very rapid, Betaine added after SLES will be unable to reach the sterically full interface. Whereas with Betaine already present the adsorption of SLES is not prevented, but is reduced and slowed.

4.4 Determination of the minimum amount of primary surfactant to be used in the preparation of the W_1/O emulsion

The minimum amount of lipophilic polymeric surfactant needed to prepare the W/O emulsion in such a way that the W/O interface is saturated can now be calculated. In emulsion preparation, as shown by Rosano[27], if enough mechanical work is provided to the system it can usually be assumed that all the surfactant molecules will be adsorbed at the W/O interface.

If **V** is the volume of the dispersed phase (W_1), and **a** the number of water droplets with an average radius **r**, then:

$$V = a \times \frac{4}{3} \pi \times r^3 \qquad (4\text{-}4\text{-}1)$$

The total interfacial area **A** produced by the formation of these W/O droplets will be equal to:

$$A = a \times 4\pi \times r^2 \qquad (4\text{-}4\text{-}2)$$

Therefore, the ratio of both equation (4-4-1)] and (4-4-2) lead the relationship:

$$A = \frac{3V}{r} \qquad (4\text{-}4\text{-}3)$$

Particle size determination was performed according to 3.2 and full results are presented in table 13. For a formulation of W1/O emulsion made of 1.5 g of PGR90, 38.5g of soybean oil and 58.5 ml of water. The average diameter of the W1 droplet was measured to be 269.8 nm.

If we assume the adsorption of one monolayer of surfactant at the W1/O interface, replacing **A** of equation **[4-4-3]** by $\underline{n \times \sigma}$ where n is the total number of molecules of surfactant and σ the molecular area occupied by a molecule of surfactant, then:

$$r = \frac{3V}{n \times \sigma} \qquad (4\text{-}4\text{-}4)$$

Therefore:

$$\sigma = \frac{3V}{n \times r} \qquad (4\text{-}4\text{-}5)$$

By substituting the data

$$\sigma = \frac{3 \times 58.5}{\frac{1.5}{1400} \times 6.02.10^{23} \times \frac{269.8}{2} \times 10^{-7}}$$

$\sigma = 201.7 Å^2$

Corresponding to this σ in figure 5 (Surface pressure correspond to 9 mN/m and a surface potential of 355 millivolts) of a monolayer of polyglycerol ester of ricinoleic acid. We are lead to the conclusion that the molecule lies flat at the O/W interface probably due to the –OH group on the ricinoleic chains (responsible for the high surface potential)

Also, in Figure 3, the polymeric surfactant starts to be compressed at an area of $0.5 m^2/mg$. Therefore using [4-4-3] we can calculate that for a

volume of dispersed phase of 20.00 ml, 0.48g of polymeric surfactant (Abil EM90®) will correspond to a diameter of the W/O droplets of 0.5µm.

4.5 Determination of the optimum amount of salt to stabilize the primary W_1/O emulsion and the $W_1/O/W_2$ double emulsion

It is necessary to add an oil-insoluble solute to the water phase to stabilize a W/O emulsion[14]. The optimum amount was determined experimentally by preparing several W/O emulsions with different amounts of salt (NaCl).

Various formulations of W/O emulsions with hexadecane as the oil phase and with different amounts of salt in the inner water phase were prepared. The lipophilic emulsifier was Abil EM90® at a concentration of 4.6% (w/w). The results showed that above a concentration of 0.3g/L of NaCl in W1, stabilization of the W/O occurs.

In the W1/O/W2 multiple emulsion, we used 0.72% (w/w) NaCl to balance the NaCl in the W2 phase brought by the Betaine. 0.72% (w/w) satisfies the requirements of stability for the W1/O emulsion. In practice, we used a chloride electrode to determine the NaCl concentration in W1 and W2.

4.6 Selecting a thixotropic water soluble polymer

Since all W1/O/W2 emulsions prepared without a thickener separate over time, we need to find a polymer with appropriate thixotropic properties[28] : one that prevents phase separation when added to our formulations, but does not interact destructively with other ingredients. We tested several hydrosoluble polymers tested for their thixotropic properties. As indicated by Figure 10, which plots the log of the viscosity of such polymers(thickeners) in water against the log of shear stress, xanthan gum and carbopol exhibit the appropriate thixotropic properties. Because of the presence of NaCl in our W1/O/W2 formulations, we also investigated the effect of NaCl on these polymers. Observing that in the presence of 1.5% (w/w) NaCl in water, carbopol lost its thixotropic properties, and xanthan gum retained them, we selected xanthan gum.

4.7 Influence of the Betaine/SLES mixture concentration on the rheological properties of XG solutions and the W1/O/W2 stability

Figure 11 plots the log of the viscosity of stable multiple emulsions against the log of shear stress. In the presence of surfactants, Betaine and

SLES were found to maintain the thixotropic properties of xanthan gum if the proportion of Betaine to SLES is at least 66% (w/w).

Above 66% of Betaine, the extrapolated viscosity at zero stress is 30 Pa.s, which is high enough to insure long range stability to the system. This is illustrated in Table 9, where the % separation of various double emulsions is given after 45 days and 220 days.

Figures 12 and 13 show the structure of a double emulsion after 1 day and 220 days. We notice no difference in size or aspect of the inner water droplets, proving that the osmotic and Laplace pressure are well balanced.

Table 6 gives the formulation of a 220 days W1/O/W2 stable emulsion in which light mineral oil is replaced by octyl palmitate and the surfactant mixture is Betaine/SDS. In Table 7, replacing Steol by SDS again yields a double emulsion stable for at least 220 days.

4.8 Droplet breakup in a double emulsion systems

The mechanisms by which various types of liquid agitation can provide the energy necessary for breakup of disperse phases have been extensively reviewed by Stroeve and Varanasi[29], Grossiord and. Seiller[30] and Lucassen-Reynders[31].

Essentially, the deformation and breakup of a droplet occurs when the stress exerted on the droplet by the flow is high enough to overcome the (O/W) interfacial cohesion due to the Laplace pressure

$$\Delta P = \frac{2\delta}{r} \qquad (4\text{-}8\text{-}1)$$

For a laminar flow, the ratio of these opposing stresses is known as the capillary number (Ca), defined by the following equation [31,32,33]:

$$Ca = \frac{\eta_c . \gamma . R}{\sigma} \qquad (4\text{-}8\text{-}2)$$

η_c= viscosity of the continuous phase

R= radius of the droplet to be broken up

σ =interfacial tension

γ = rate of shear

In order for the droplet to break into fragments, it is necessary for the droplet to elongate sufficiently. This implies that the hydrodynamic shear has to exceed the cohesion constraint due to capillary forces. The division of droplets has been discussed by Rumscheidt and Mason [34]. They found, experimentally, that droplets break up into two or more segments when the capillary number Ca exceeds a critical value, Ca_{cr} .

Experimentally, Ca_{cr} is found to depend on the type of flow and on the viscosity ratio of the two liquids. The critical value of Ca_{cr}, according to Grossiord and Sellier[30], must be around 1.

When discussing the formation of single or double emulsions, the role of the surfactant has to be recognized. When an O/W interfacial area increases rapidly, the interfacial tension rises and conditions favor droplet recoalescence. In regards to interfacial viscosity, it is role is difficult to measure and thus is generally ignored.

So, when discussing single emulsion formations, only one type of droplet fragmentation is to be considered: either W/O or O/W.

With double emulsions two types of droplet fragmentation should be considered:

1- *the fragmentation of the of the* W1/O droplets in W2

2- the fragmentation of the W1 droplets in O

Therefore, the analysis of the droplet break up in double emulsion systems is quite complicated. We tried to explain a certain number of experimental results listed in table 12 (which is a series of observations on double emulsions using the basic formulation).

Experimentally, viscosity of the W2 phase is necessary to emulsify W1/O in W2, as can be seen in experiment number 5,3, 8 in Table 12. Even when W2 is sufficiently viscous, SLES and SDS are too efficient emulsifiers, due most probably to the penetration at the O/W interface and the transitional lowering of the interfacial tension. Betaine being more of an oil

dispersant, does not seem to affect the W1/O emulsion. Finally, in order to obtain long term stability the system has to be thixotropic - the role played by the xanthan gum.

5. Dynamic Interfacial Tension

5 Measurement of the dynamic interfacial tension oil/water using the Pendant Drop Tensiometer method.

5.1 The Pendant Drop Technique

To measure the dynamic interfacial tension, the pendant drop technique was used. In this technique a drop of oil, *n-hexadecane*, is formed from a needle tip into the surfactant solution of water. The surface tension of the drop is determined by the drop shape. This technique is known to be clean interface adsorption and re-equilibration. With a clean interface adsorption, oil/water, the droplet is impulsively formed in the aqueous solution and the reduction in tension is measured as the surfactant adsorbs into the interface. Aqueous solutions are prepared using water from a Milli-Q water purification system. This technique will allow to understand the difference in behavior observe for SLES and betaine when used as a secondary surfactant in the outer aqueous phase W2. Bruno and al.[35] have investigated the same phenomena with SDS using neutron reflectivity measurements.

5.2 Equilibrium Adsorption Measurement and Discussion

With the use of this technique, dynamic interfacial tensions were measured between an oil phase of n-hexadecane (with and without Abil Em 90). The water phase contained SLES and betaine (concentration: 10^{-4} M) and a 50/50 mixture of both surfactants.

Figure 14 shows the dynamic surface tension relaxation for adsorption into a clean interface for three aqueous solutions (Betaine, SLES and mixture). The time, t = 0, in these relaxations represents the point at which the hexadecane droplet growth is terminated. From figure 14, it is possible to explain the difference in the behavior observed when betaine and SLES are used as the surfactant in W2. With betaine, we observe a higher droplet size of W1/O/W2 than with SLES. Figure 14 shows that the interfacial tension drops more rapidly and to a lower interface tension with SLES (9.0 mN) than with Betaine (18.0 mN). Due to a lower interfacial tension between the oil phase and the water phase when SLES is used rather than Betaine, smaller droplets of W1/O/W2 are expected and will eventually result in a single emulsion (O/W).

Figure 15 demonstrates the sequence in which the double emulsion are made. In the first step, Betaine has to be added first into W2 because use of SLES or the mixture will result in smaller droplets and a single emulsion. In the second step, when SLES is added, we observe a reduction of the size of the droplet W1/O/W2 due to a reduction of the interfacial tension between W1/O and W2 (Figure 15).

6.Theoretical Approach of the Effect of an oil-insoluble Solute on the Stability of Multiple water-oil-water Emulsion

6 Theoretical approach of the effect of an oil-insoluble Solute on the stability of multiple water-oil-water emulsion

6.1 A Model for the behavior of two W/O droplets (or G/W *bubbles) containing a solute (or a gas) insoluble in the continuous phase.*

This model covers both the case of two water-in-oil droplets and that of two gas-in-water bubbles. For simplicity, we present the model as applied to the case of two droplets of saline solution dispersed in a solvent.

6.1.1 Flux of water due to the Laplace pressure between two droplets dispersed in a solvent.

We consider two water droplets of radii r_1 and r_2, $r_1 < r_2$, dispersed in a solvent (the continuous phase), and we assume that water is only sparingly soluble in this solvent. Let γ equal the interfacial tension (assumed to be constant) and C_m the concentration of solvent in the continuous phase.

Kabalnov and Shchukin [36] used a Kelvin equation to express the increase in solubility of a substance inside spherical particles as the size of these particles diminishes:

$$C(r) = C(\infty)\, e^{\frac{2\gamma V_m}{RTr}} \approx C(\infty)\left(1 + \frac{2\gamma V_m}{RTr}\right) \qquad (6\text{-}1\text{-}1)$$

where C(r) is the solubility of the dispersed solvent in the continuous phase at the surface of a droplet of radius r, $C(\infty)$ is the solubility of this same solvent in the continuous phase but with a flat interface, and V_m is the molar volume of the solvent (water).

Due to the Laplace pressure, the solubility of water in the interfacial region around the smaller droplet (r_1) is larger than the solubility of water in the solvent between the two droplets. A water gradient of concentration is created in the continuous phase. After a certain time, the concentration of water in the continuous phase is larger than the concentration of the water at the interface of the larger droplet (r_2), and water enters the larger droplet.

After a while, the flux of water leaving the smaller droplet equals the flux entering the larger one. Using Fick's law at the interface of each droplet, as Princen[37] did for the diffusion of a gas in a soap film, we can express

the relation between the gradient of concentration at the surface of each droplet and the radii:

$$J_1 = J_2 \qquad \text{with} \quad J_i = -4\pi r_i^2 D \frac{\partial c}{\partial r}\Big|_{r=r_i} \text{ (Fick's law)} \quad (6\text{-}1\text{-}2)$$

$$-4\pi r_1^2 D \frac{\partial c}{\partial r}\Big|_{r=r_1} = -4\pi r_2^2 D \frac{\partial c}{\partial r}\Big|_{r=r_2}$$

$$r_1^2 \frac{\partial c}{\partial r}\Big|_{r=r_1} = r_2^2 \frac{\partial c}{\partial r}\Big|_{r=r_2} \quad (6\text{-}1\text{-}3)$$

where r_1 and r_2 represent the radii of the two droplets and D is the water diffusion coefficient in the continuous medium.

If the gradient of the water concentration in the interfacial region (of thickness δ) decreases linearly, and assuming the same value of δ for the two droplets, this gradient may be expressed as follows:

$$\frac{\partial C}{\partial r}\Big|_{r=r_1} = \left(\frac{C_m - C(r_1)}{\delta}\right) \text{ and } \frac{\partial C}{\partial r}\Big|_{r=r_2} = \left(\frac{C(r_2) - C_m}{\delta}\right) \quad (6\text{-}1\text{-}4)$$

From equations (6-1-3) and (6-1-4), the equality of the two fluxes may be expressed as:

$$r_1^2\left(\frac{C(r_1)-C_m}{\delta}\right)=r_2^2\left(\frac{C_m-C(r_2)}{\delta}\right) \qquad (6\text{-}1\text{-}5)$$

and C_m can be expressed as a function of the two radii r_1 and r_2:

$$C_m=\frac{r_1^2C(r_1)+r_2^2C(r_2)}{r_1^2+r_2^2} \qquad (6\text{-}1\text{-}6)$$

Therefore, the flux of water going through the interfacial regions surrounding the two droplets can be expressed as:

$$J_L=-4\pi r_1^2 D\frac{(C_m-C(r_1))}{\delta} \qquad (6\text{-}1\text{-}7)$$

using equation (6-1-6) and replacing $C(r_1)$ and $C(r_2)$ by their values found through Kabalnov's equation (6-1-1), the Laplace flux becomes:

$$J_L=\frac{4\pi r_1^2 r_2^2 D\alpha C(\infty)}{\delta\left(r_1^2+r_2^2\right)}\left[\frac{1}{r_1}-\frac{1}{r_2}\right] \qquad (6\text{-}1\text{-}8)$$

with $\alpha=\frac{2\gamma V_m}{RT}$ (which has the dimension of length).

The radius r_1 being smaller than the radius r_2, J_L, as written above, takes a positive value.

6.1.2 Flux of water between the two water droplets due to the osmotic pressure.

If the two droplets contain a concentration $\mathbf{m_o}$ (moles/liter), a solute soluble in the dispersed phase but totally insoluble in the continuous phase (in the present case NaCl), we can conceive a difference in osmotic pressure between the two droplets, as the smaller will decrease in size and the larger will increase, due to the Laplace pressure effect.

The solvent separating the two droplets can be considered as a homogenous liquid membrane, and the flux, per unit of interface, due to the osmotic pressure can be expressed as follows:

$$J_o = -L_o(\Delta P) = -L_o RT(\Delta C) \qquad (6\text{-}1\text{-}9)$$

where L_o is an overall permeability constant (consistent with the definition given by Lemlich [38] of the permeability of the continuous phase having the dimension of a diffusion coefficient divided by a length, divided by RT. L_o is a result of the resistance across the two interfaces and across the liquid lamella separating the two droplets (we assume, as in Section 1 above, that the resistance to the migration of waterin the membrane of the liquid lamella,

compared to that of the interfaces, is negligible, because of the greater gradient of concentration in the interfaces). ΔP is the difference between the osmotic pressures of the two droplets.

Replacing ΔP by the van't Hoff expression for the osmotic pressure, we find that the concentration of the solute in a droplet is equal to the initial number of moles present divided by the volume of the droplet at a time t:

$$C = \frac{\left(m_o \times \frac{4\pi r_0^3}{3}\right)}{\frac{4\pi r_t^3}{3}} = m_o \times \frac{r_0^3}{r_t^3} \qquad (6\text{-}1\text{-}10)$$

where r_O is the initial radius of a droplet and r_t is the radius at a later time t.

So, from equations (6-1-9) and (6-1-10), we can express the flux between the two droplets of radius r_1 and r_2, $r_1 < r_2$, as

$$J_o = -L_o RT(C_1 - C_2) = -L_o RT\, m_o \left(\frac{r_{o1}^3}{r_1^3} - \frac{r_{o2}^3}{r_2^3}\right)$$

$$J_o = -L_o RT\, m_o\, r_{o2}^3 \left(\left(\frac{r_{o1}}{r_{o2}}\right)^3 \frac{1}{r_1^3} - \frac{1}{r_2^3}\right)$$

where r_{o1} and r_{o2} are the initial radii of the droplets 1 and 2. If we set θ equal to the ratio of the radii of the two droplets, we obtain a final expression:

$$J_o = -L_o RTm_o r_{o2}^3 \left(\theta^3 \frac{1}{r_1^3} - \frac{1}{r_2^3} \right) \text{ with } \theta = \frac{r_{o1}}{r_{o2}} \leq 1 \qquad (6\text{-}1\text{-}11)$$

Considering the surface of the smaller droplet as the limiting surface for the osmotic flux., we can then express the total flux due to the osmotic pressure as:

$$J_{oT} = 4\pi r_1^2 J_o = -4\pi L_o RTm_o r_{o2}^3 r_1^2 \left(\theta^3 \frac{1}{r_1^3} - \frac{1}{r_2^3} \right) \qquad (6\text{-}1\text{-}12)$$

As the size of the smaller droplet decreases and the size of the bigger one increases, C_1 is superior to C_2, and the osmotic flux, as written, takes a negative value.

6.1.3 Total flux of water (dispersed phase), between two droplets containing an insoluble solute (NaCl) dispersed in a continuous phase, in terms of Laplace and osmotic fluxes.

Using the separate expressions for Laplace and osmotic fluxes that we have established in equations (6-1-8) and (6-1-12), we may write the total flux as follows:

$$J_T = J_L + J_{oT}$$

$$J_T = \frac{4\pi r_1^2 r_2^2 D\,\alpha C(\infty)}{\delta(r_1^2 + r_2^2)}\left[\frac{1}{r_1} - \frac{1}{r_2}\right] - 4\pi L_o RT m_o r_{o2}^3 r_1^2\left(\theta^3\frac{1}{r_1^3} - \frac{1}{r_2^3}\right)$$

(6-1-13)

We abbreviate the coefficient of each term in (6-1-13) in order to simplify the writing of this equation.

$$K_L = \frac{4\pi D\,\alpha C(\infty)}{\delta} \qquad \text{and} \qquad K_o = 4\pi L_o RT m_o r_{o2}^3$$

Given the conservation of matter, the quantity $(C_m + V_o)$, where Vo is the total initial volume, is constant.

Assuming that the quantity of water dissolved in the continuous phase is very small and varies little, we can express the conservation of matter for the system by considering only the total volume of the two droplets. So, at any instant, the state of the system is:

$$V_o = \frac{4\pi r_{01}^3}{3} + \frac{4\pi r_{02}^3}{3} = \frac{4\pi r_1^3}{3} + \frac{4\pi r_2^3}{3}$$

The radius r_2 may thus be expressed as a function of r_1 only:

$$r_2 = \sqrt[3]{\Omega - r_1^3}\ , \text{ with } \Omega = \frac{3V_o}{4\pi}$$

And equation (6-1-13) becomes:

$$J_T = K_L \frac{r_1^2(\Omega - r_1^3)^{\frac{2}{3}}}{\left(r_1^2 + (\Omega - r_1^3)^{\frac{2}{3}}\right)}\left[\frac{1}{r_1} - \frac{1}{(\Omega - r_1^3)^{\frac{1}{3}}}\right] - K_o r_1^2\left(\theta^3 \frac{1}{r_1^3} - \frac{1}{(\Omega - r_1^3)}\right)$$

(6-1-14)

6.1.4 Visualizing the role played on the equilibrium by the concentration of the insoluble substance within the droplets.

6.1.4.1 Determining the parameters K_L, K_O:

$$K_L = \frac{4\pi D \alpha C(\infty)}{\delta} \approx 1.25*10^{-20} \text{ mol.cm}^{-1}.\text{s}^{-1}$$

if we assign the following values to the different constants:

D, the diffusion coefficient at the interfaces, $= 10^{-5}$ cm^2.s^{-1}

$\alpha = 10^{-7}$ cm

$C(\infty)$, the solubility of the dispersed phase in the continuous one,$= 10^{-15}$ mol.cm^{-3}

δ, the length of the diffusion layer,$= 10^{-6}$ cm

$$K_o = 4\pi L_o R T m_o r_{o2}^3 \approx 1.25.10^{-20} \text{mol.cm.s}^{-1}$$

if, in calculating L_o, the overall permeability of the interbubble medium (diffusion coefficient divided by a thickness and divided by RT), we set the diffusion coefficient $D \approx 10^{-5}$ $cm^2.t^{-1}$ and use a thickness of $\approx 10^{-5}$ cm, we have $\approx 10^{-2}$:

and setting m_o, variable $\approx 10^{-6}$ $mol.cm^{-3}$

and $r_{o2} \approx 10^{-5}$ cm

It is clear that we cannot know the exact values of these two parameters, but the above approximation allows us to assign very similar values to them.
We end up treating the evolution of the total flux of water between the two droplets as a function solely of the radius of the smaller one. It is obvious that equilibrium will be reached when the total flux is equal to zero. In turn, the zero value of the flux gives us the radius of the smaller droplet at equilibrium.

6.1.4.2 Evolution of the total flux between the two droplets as the radius r_1 diminishes:

Relative Flux (Total Flux/Initial Flux)

The three curves plotted in Figure 16 above correspond to three different initial droplet-radius ratios. As the initial difference between the sizes of the droplets increases, the initial flux, due essentially to the difference in Laplace pressure, increases. We also see that the greater the initial difference, the smaller the droplet will be at equilibrium, because the system requires a greater evolution in size to permit the osmotic flux to counterbalance the initial Laplace flux.

Relative flux of water

Since K_o is proportional to the concentration of the solute in the dispersed phase, we can visualize the effect of the concentration on the evolution of the system just by considering the flux as a function of r1, for different values of K_o.

When K_o is equal to zero, we have the disappearance of the smaller bubble or droplet due to the Laplace pressure difference. When we take a non-zero value for K_o, we find a zero flux for a non-zero radius r_1, the equilibrium radius.

The plots of the curve for K_o=1 and K_o=10 (Fig. 18) show the tremendous effect of the concentration on the final size of the droplet. Indeed, the equilibrium radius will be 0.4 r_{o1} for K_o=1 and 0.9 r_{o1} for K_o=10.

6.1.4.3 Limits of the model

For the purposes of simulation, we assume that the system is in a steady state, which implies that the variation of C_m is not important and does not create a large gradient of concentration in the continuous medium.

Figure 18 allows us to verify that the assumption is valid only in cases in which the droplet does not disappear. In such a case, the exponential included in the expression (6-2-6) for the solubility at the interface of the smaller droplet becomes predominant, giving rise to a rapid increase in Cm. In any event, Equation (6-2-14) cannot be used for the disappearance of a droplet, since in this case the exponential of the Kelvin equation cannot be given a first-order approximation.

Therefore, such other physical events as the desorption of the surfactant from the interface must be taken into account. To sum up, as shown in Figure18, we can apply the model if we consider a diminution in size down to, but not beyond, a radius of a few nanometers, which corresponds to the evolution of the system when balanced by osmotic pressure as in Figures 17 and 18.

6.2 Predicting Changes in Bubble-Size Distribution due to Interbubble Gas Diffusion in Foams.

6.2.1 The Theory of Lemlich

At least two distinct spontaneous phenomena can change an existing distribution of bubble sizes in a liquid foam: one involves the rupture of the lamellae between bubbles, another the transfer of gas between bubbles by diffusion. While some liquid foams are extremely resistant to the first phenomenon, i.e., to rupture, none are immune to the second. The following treatment of interbubble gas diffusion and resultant change in bubble-size distribution builds on the work of Lemlich[39]. Lemlich's approach, instead of viewing the gas as diffusing directly from bubble to bubble, sees it as first diffusing into the liquid region midway between the bubbles. The concentration of gas in this liquid can be considered as being equivalent (through Henry's law) to a gas pressure in the liquid. Then, by virtue of the law of Laplace and Young, this gas-pressure equivalent can be considered to be the gas pressure that would exist within a hypothetical spherical bubble of radius ρ. Thus the pressure difference ΔP_{Lap} between a bubble of any radius r and the liquid is

$$\Delta P_{Lap} = 2\gamma\left(\frac{1}{\rho} - \frac{1}{r}\right) \qquad (6\text{-}2\text{-}1)$$

where γ is the surface tension.

The molar rate of gas transfer S(r,t) from a bubble to the liquid is assumed to be given by :

$$S(r,t) = -JA\Delta P_{Lap} \qquad (6\text{-}2\text{-}2)$$

where J is the effective permeability of the continuous phase to the transfer and A is the surface area through which the transfer takes place. If n is the number of moles of gas in the bubble, by the conservation of moles we have

$$S(r,t) = -\frac{dn}{dt}$$

and if we approximate A by $4\pi r^2$, Equations (6-2-1) and (6-2-2) yield

$$\frac{dn}{dt} = 8\pi J\gamma\left(\frac{r^2}{\rho} - r\right) \qquad (6\text{-}2\text{-}3)$$

By assuming conservation of gaseous moles throughout the foam as a whole, $\sum_i \frac{dn}{dt} = 0$. The summation is taken over all the bubbles. Using (6-2-3), we get

$$\sum_i n_i\left(\frac{r_i^2}{\rho} - r_i\right) = 0 \quad (6\text{-}2\text{-}4)$$

where n_i is the number of bubbles of radius r_i.

Lemlich carried this approach further and considered an average effective ρ, independent of r but varying with time. Thus, (6-2-4) gives

$$\rho = \frac{\sum_i n_i r_i^2}{\sum_i r_i} \quad \text{or} \quad \rho = \frac{\int_0^\infty r^2 F(r,t)dt}{\int_0^\infty rF(r,t)dt} \qquad (6\text{-}2\text{-}5)$$

where F(r,t) is the frequency distribution function of r at time t.

Furthermore, as the pressure in a bubble is only slightly higher than the surrounding pressure P_a , which is typically the atmospheric pressure, from the ideal gas law and the formula for the volume of a sphere

$$n = \frac{4\pi P_a r^3}{3R_g T} \qquad (6\text{-}2\text{-}6)$$

where R_g is the ideal gas constant and T is the absolute temperature.

Combining Equations (6-2-3), (6-2-5), and (6-2-6) Lemlich deduced that the rate of change of the radius of a bubble over time is given by

$$\frac{dr}{dt} = \frac{2J\gamma R_g T}{P_a}\left(\frac{\int_0^\infty rF(r,t)dt}{\int_0^\infty r^2F(r,t)dt} - \frac{1}{r} \right) \qquad (6\text{-}2\text{-}7)$$

or more succinctly

$$\frac{dr}{dt} = K\left(\frac{1}{r_{21}} - \frac{1}{r} \right) \qquad (6\text{-}2\text{-}8)$$

where $K = \frac{2J\gamma R_g T}{P_a}$ and $r_{21} = \frac{\int_0^\infty r^2F(r,t)dt}{\int_0^\infty rF(r,t)dt}$ .Thus bubbles with $r > r_{21}$ grow in size, whereas bubbles with $r < r_{21}$ shrink in size and eventually disappear.

For the sake of generality and utility in simulations, Equation (6-2-8) is recast in a dimensionless form as

$$\frac{dR}{dY} = \left(\frac{1}{R_{21}} - \frac{1}{R} \right) \qquad \text{with} \qquad R = \frac{r}{r_c} \qquad Y = \frac{Kt}{r_c^2}$$

where r_c is some convenient characteristic radius such as the average initial radius of the distribution.

6.2.2 Lemlich's theory applied to a bubble containing a gas insoluble in the continuous phase

If the gas bubbles initially contain a certain amount of gas totally insoluble in the continuous phase, then as the bubbles change in size an osmotic pressure will develop between them. If we consider the phenomenon with two bubbles of different initial radius, initially the concentration of the insoluble vapor is constant and only the Laplace pressure acts. Thus the smaller bubble shrinks and the larger one increases in size. As a consequence of the changes in size, the concentration of insoluble gas increases in the smaller bubble and decreases in the larger one, giving rise to an osmotic pressure opposite the Laplace pressure.

The osmotic pressure difference ΔP_{osm} that drives a flux of the soluble gas opposite the flux driven by the Laplace pressure difference can be written as:

$$\Delta P_{osm} = R_g T \Delta m$$

where R_g is the gas constant, T the absolute temperature, and Δm the difference in concentration of the insoluble gas between the fictitious bubble of radius ρ and a bubble of radius r.

Using m_o as the initial concentration of insoluble gas, and r_o and ρ_o as the initial radii of the bubble and the fictitious bubble, respectively, we get

$$\Delta P_{osm} = m_o R_g T\left(\left(\frac{r_o}{r}\right)^3 - \left(\frac{\rho_o}{\rho}\right)^3\right) \qquad (6\text{-}2\text{-}9)$$

Recalling Equation (6-2.2), we have

$$S(r,t) = -JA\left(\Delta P_{Lap} + \Delta P_{Osm}\right) \qquad (6\text{-}2\text{-}10)$$

The conservation of the total number of moles of the soluble gas gives

$$\sum_i n_i\left(\frac{r_i^2}{\rho} - r_i\right) + \frac{m_o R_g T}{2\gamma}\sum_i n_i\left(\frac{r_{io}^3}{r_i} - \frac{\rho_o^3}{\rho^3} r_i^2\right) = 0 \qquad (6\text{-}2\text{-}11)$$

Assuming that ρ is independent of r but varies with time, (6-2-11) would yield a cubic equation for ρ as a function of the initial radius and at

time t. Without pursuing this line of reasoning, we note only that ρ is initially equal to r_{21}, and for the purpose of the following discussion we will assume that ρ has this value.

From (6-2-9) and (6-2-10), following Lemlich[38], we derive the rate of change of the radius time:

$$\frac{dr}{dt} = \frac{2J\gamma R_g T}{P_a}\left[\frac{1}{r_{21}} - \frac{1}{r} + \frac{m_o R_g T}{2\gamma}\left(\left(\frac{r_o}{r}\right)^3 - \left(\frac{r_{21o}}{r_{21}}\right)^3\right)\right]$$

(6-2-12)

For the sake of generality and utility in simulations, Equation (6-2-12) is recast in a dimensionless form as

$$\frac{dR}{dY} = \frac{1}{R_{21}} - \frac{1}{R} + \Phi\left(\left(\frac{R_o}{R}\right)^3 - \left(\frac{R_{21o}}{R_{21}}\right)^3\right) \qquad (6\text{-}2\text{-}13)$$

with $$R = \frac{r}{r_c} \qquad Y = \frac{2J\gamma R_g T}{P_a}\frac{t}{r_c^2} \qquad \Phi = \frac{m_o R_g T r_c}{2\gamma}$$

where r_c is some convenient characteristic radius, such as the average initial radius of the distribution.

6.2.3 Numerical simulation

6.2.3.1 Values for R_{21} and Φ

For values typically found in familiar liquid foams -- m_o = 0.01 mol/L, γ = 30 dynes/cm, T = 298 °K, and r_c = 1μm -- we have Φ = 0.4. With this example in mind, we see that a reasonable range of values to investigate for Φ is between 0.01 and 1.

Beginning with the empirical distribution of de Vries and the Maxwell-Boltzmann-like distribution of Bayens, we can determine the following initial values of R_{21}: 1.48 for the distribution of de Vries and 1.18 for the distribution of Bayens.

6.2.3.2 Curves of dR/dY as a function of R

Using Equation (6-2.13), and assuming that R_{21} is a constant equal to its initial value, we can plot dR/dY as a function of R if we know the initial value of the radius of a bubble . Figure 21 shows one such plot for $R_o < R_{21}$. We start with an initial radius (R_o) of 0.6. At this radius dR/dY is

negative, so the radius will decrease. This initial decrease is due to the Laplace pressure; as the minimum value of dR/dY is reached, the osmotic pressure becomes more significant, equalling and then exceeding the Laplace pressure, with a resultant rapid decrease in dR/dY to a value of 0. This equilibrium is a stable one, because if the bubble continues to shrink, dR/dY becomes positive and the radius increases again.

Figure 22 shows the difference in the initial rate of shrinkage for bubbles with different initial radius. We see that the smaller the bubble, the greater the Laplace pressure. For initial radii of 0.6, 0.9, and 1.3, the equilibrium radii are 0.107, 0.204, and 0.378, respectively.

6.2.3.3 Influence of the amount of insoluble gas

Figure 23 shows the effect of increasing the osmotic pressure on dr/dt. As can be seen, as we increase Φ we reduce the effect of the Laplace pressure,while the equilibrium radius increases as well. Figure 20 shows that an increase in Φ also leads to an equilibrium radius closer to the initial radius.

6.2.3.4 Variation of the radius as a function of time

As Monsalve and Schechter[39] showed, if we assume R_{21} to be constant, then the equation of Lemlich (6-2-8) (which is Equation (6-2-12) with $\phi = 0$), can be integrated to give :

$$Y = R_{21}\left(R - R_o + R_{21} \mathrm{Ln}\left(\frac{R - R_{21}}{R_o - R_{21}} \right) \right)$$

We can then plot Y as a function of R (or vice versa R as a function of Y), as shown in Figure 24.

If we wish to take into consideration the contribution of an osmotic pressure (i.e., $\Phi \neq 0$), we integrate the equation numerically (using Mathematica) and plot R as a function of time: see Figure 24. This figure shows clearly that adding a small amount of insoluble compound prevents the bubble from disappearing, and an equilibrium radius is attained.

6.2.3.5 Is the hypothesis of constant R_{21} reasonable ?

As can be seen from Fig. 25, a change in R_{21} has very little effect on the curves for dR/dY. Thus, the hypothesis of constant R_{21} is tenable, at least for $R_o < R_{21}$.

6.2.4 Stable equilibrium condition

The conditions necessary for one bubble of radius r to reach a stable equilibrium are (i) that $\frac{dr}{dt} = 0$ and (ii) that $\frac{d^2r}{dt^2} \leq 0$.

Let us expand the second condition, taking into consideration the fact that r_{21} is a function of time.

$$\frac{d^2r}{dt^2} = K\left(-\frac{1}{r_{21}^2} + 3\frac{m_o R_g T}{2\gamma}\left(\frac{r_{21_o}}{r_{21}}\right)^3 \frac{1}{r_{21}}\right)\frac{dr_{21}}{dt}$$

As $\frac{dr_{21}}{dt} \geq 0$, the condition $\frac{3m_o R_g T r_{21_o}^2}{2\gamma} \leq r_{21}^2$

must be fulfilled.

6.3 Equilibrium of a water in oil droplet containing a certain amount of salt.

We consider a water droplet of radii r containing a certain amount of salt, in a solvent (oil phase), and we assume that the film around this water droplet prevents coalescence but is not impermeable to water.

The Laplace pressure $\frac{2\gamma}{r}$ of a droplet containing a salt, dispersed in a solvent, will increase the shrinkage of the droplet, while the osmotic pressure will increase as well, leading in turn to a reduction in activity of the diffusible solvent (water in the present case) and thus stimulating back-diffusion of the solvent. In the ideal case, the osmotic pressure is given by:

$$\Pi_{osm} = mRT = m_o \left(\frac{r_o}{r} \right)^3 RT$$

where m is the molar concentration of salt and m_o refers to the original droplet.

Let us write the excess pressure ΔP in the droplet as:

$$\Delta P = \frac{2\gamma}{r} - m_o \left(\frac{r_o}{r} \right)^3 RT$$

At equilibrium, we should have:

$$\frac{d(\Delta P)}{dr} = -\frac{2\gamma}{r^2} - 3m_o\left(\frac{r_o}{r}\right)^3 \frac{1}{r} RT = 0$$

Thus, $2\gamma \leq 3mRTr$ (6-3-1)

Using equation (6-3-1), which has been proposed by Walstra [40], we may calculate the minimum percentage difference of NaCl required (for various values of the radius of the droplet and a surface tension of 10mN/m.) to counterbalance the Ostwald ripening between two droplets; these values are listed in Table 14. Another condition is that m has to be greater than 2γ/ 3RTr. It is apparent that very small quantities of a suitable solute will suffice to stop Ostwald ripening.

6.4 Conclusion

Despite the simplicity of our model, it is clear that the presence of a small quantity of an insoluble solute, in the case of a water-in-oil dispersion (or of an insoluble vapor, in the case of a foam), may prevent the destabilizing effect of the Ostwald ripening phenomenon.

It appears that, following the changes in radius of the two bubbles, a difference in salt concentration on the order of 0.0016% to 0.0004% for a

radius of 100 to 400 nm will be sufficient to stop Ostwalt ripening (when $\gamma =$ 10 mN/m).

7. Conclusion

7 Conclusion

New protocols enabling preparation of $W_1/O/W_2$ double emulsions have been achieved and presented in this paper, one using soy bean oil with edible ingredient and another containing 15% (w/w) of surfactants in the external phase. Previously, both theoretical and experimental approaches to the stability of W1/O/W2 multiple emulsions had been studied , though incompletely. The theoretical approach emphasized the role of Ostwald ripening in countering stability in W/O emulsions. It also discussed the addition of an oil-insoluble solute to the inner water phase of the system in order to produce an osmotic pressure opposed to the Laplace pressure. The previous studies assumed complete stability of the W1/O/W2 adsorbed interfacial films. However, our studies demonstrate that after several low HLB surfactants were tested, only three were found to produce stable W1/O emulsions.

1) cethyl dimethicone copolyol (Abil Em90-*ICI*)
2) A-B-A block copolymer (Arlacel P135-*Rhodia*)
3) polyglycerol ester of ricinoleic acid (Grinstead PGR90- *Danisco*)

The results obtained from our monolayers studies show that certain conditions need to be attained in order to reach stable interfacials film, W1/O and O/W2. We found the following:

1. The film formed by the low HLB surfactant at the W1/O interface should be reversibly expandable and compressible, and irreversibly adsorbed.

2. The long term stability of the double emulsion requires a balance between Laplace and the Osmotic Pressure (between W1 droplets in Oil). Our theoretical approach and experimental results seem to explain how a small quantity of salt in the water-in-oil droplets is able to balance, by osmotic opposition the Laplace pressure.

   Videomicroscopic observations of the multiple emulsions vs. time make it possible to determine the right salt concentration necessary to balance osmotic pressure between the two water phases.

3. The presence of a thickener is necessary in the outside phase in order to reach a viscosity ratio (preferentially around 1) of both phases (W1/O and W2), allowing dispersion of the viscous primary emulsion into the W2 aqueous phase. Also the thixotropie property of the thickener prevents from phase separation.

4. The interactions between the low and high HLB emulsifiers at the O/W_2 interface should not destabilize the films. If an aggressive surfactant such as SLES (or, presumably, SDS) is used at high concentration in $W_1/O/W_2$ multiple emulsions, the preferred method of emulsion preparation will include the following: a) to emulsify the W_1/O with Betaine F, which

tolerates a relatively vigorous mechanical work (Ultra-Turrax), and b) to add the second surfactant using mild mechanical work (under 1000 rpm, mechanical stirrer). The amount of mechanical work applied to the system will determine the size of the oil droplets.

Carbohydrates	**Surfactants**
Acacia	Anionic
Agar	Cationic
Chondrus	Nonionic
Pectin	Solids
Tragacanth	Aluminum hydroxide
Proteins	**Bentonite**
Casein	**Magnesium hydroxide**
Egg yolk	
Gelatin	**High Molecular Weight Alcohols**
	Cetyl alcohol
	Glyceryl monostearate
	Stearyl alcohol

Table 1: Emulsifiers and Stabilizers for Emulsions Carbohydrates Surfactants

Acacia Acacia **12.0**	Tween 20 Polyoxyethylene sorbitan monolaurate **16.7**
Glyceryl monostearate **3.8**	Tween 21 Polyoxyethylene sorbitan monolaurate **13.3**
Methocel 15 cps Methylcellulose **10.5**	Tween 40 Polyoxyethylene sorbitan monopalmitate **15.6**
PEG 400 Monoleate Polyoxyethylene **11.4**	Tween 60 Polyoxyethylene sorbitan monostearate **14.9**
PEG 400 Monostearate Polyoxyethylene **11.6**	Tween 61 Polyoxyethylene sorbitan monostearate **9.6**
PEG 400 Monolaurate Polyoxyethylene **13.1**	Tween 65 Polyoxyethylene sorbitan tristearate **10.5**
Parmagel B Gelatin **9.8**	Tween 80 Polyoxyethylene sorbitan monooleate **15.0**
Potassium oleate **20.0**	Tween 81 Polyoxyethylene sorbitan monooleate **10.0**
Na lauryl sulfate / Na lauryl sulfate **40.0**	Tween 85 Polyoxyethylene sorbitan trioleate **11.0**
Na oleate **18.0**	
Span 20 Sorbitan monolaurate **8.6**	
Span 40 Sorbitan monopalmitate **6.7**	
Span 60 Sorbitan monostearate **4.7**	
Span 65 Sorbitan tristearate **2.1**	
Span 80 Sorbitan monooleate **4.3**	
Span 85 Sorbitan trioleate **1.8**	
Tragacanth Tragacanth **13.2**	
Triethanolamine oleate **12.0**	

Table 2:HLB Values of Emulsifiers: Commercial Name, Chemical Name and HLB Value

Ascorbic acid	4-Hydroxymethyl-2, 6, -di-tert-butylphenol
Ascorbyl palmitate	Propyl gallate
Butylated hydroxyanisole	Sulfites
Butylated hydroxytoluene	L-Tocopherol
Gallic acid	

Table 3: Antioxidants for Emulsions

Beeswax **12**	Paraffin wax **11**
Cetyl alcohol **15**	Petrolatum **12**
Cottonseed oil **10**	Stearic acid **15**
Lanolin, anhydrous **10**	Stearyl alcohol **14**
Mineral oil, light/heavy **12**	

Table 4: Required HLB Values for Some Common Lipid Material to Prepare o/w Emulsions

		Composition %(w/w)
W_1	H_2O	59.6
	NaCl	0.40
Oil	Soy bean Oil	36.0
	Low HLB surfactant	4.0

Table 5: Preparation of several W_1/O emulsions with different low HLB surfactant in W1.

		Composition %(w/w)
W_1	H_2O	58.5
	NaCl	0.4
	Acetic Acid	pH=4
Oil	Soy Bean Oil	36
	Low HLB surfactant	4.0
	37.5g of W1/O	inW2
W_2	H_2O	61.25
	High HLB surfactant	0.525
	NaCl	0.5
	Acetic Acid	pH=4
	Xanthan gum	0.6

Table 6: Standard Formulation for W1/O/W2 Using Tween 60 as High HLB surfactant.

		Composition %(w/w)
W_1	H_2O	18.78
	NaCl	0.72
Oil	Light mineral Oil	10.02
	Low HLB surfactant	0.48
W_2	H_2O	19.6
	Tego Betaine F®	50-X
		(14.7-Y Betaine)
	Steol CS-330®	X
		(Y SLES)
	Xanthan gum	0.4

Table 7: Standard Formulation for W1/O/W2 when using SLES and Betaine as High HLB surfactant.

Surfactant	HLB	Stability of the emulsion 1 month @room temperature
Mono and diglyceride: (BFP 75)		Not Stable
Hexaglyceryl tetraoleate (Poly.6-4-0)	5	Not Stable
Decaglyceryl decaoleate (Poly.10-10-0)	3	Not Stable
Polyglycerol esters of ricinoleic acid (PGR)	2	Stable
Polyglycerol esters of fatty acids (PGE)	3	Not Stable
Decaglyceryl x-oleate (ADM Caprol ET)		Not Stable
Fluid lecithin from mixed phospholipid (Actiflo.)	2	Not Stable
Cethyl dimethicone copolyol (Abil Em90)		Stable
Sorbitan monosterate (span 60)		Not Stable
Sorbitan tristerate (span 65)	4.7	Not Stable
Sorbitan monooleate (Crillet NF)	2.1	Not Stable
A-B-A block copolymer (Arlacel P135)		Stable

Table 8: The different classes of primary surfactant (low HLB) tested for their ability to produce a stabilize W/O emulsion. Formulated according to Table 3.

% Betaine (w/w) (Betaine/SLES mixture)	% Separation after 220 days @ RT + Xanthan Gum	% Separation after 45 days @ RT - Xanthan Gum
0	43.7	62.4
14	45.0	62.0
30	50.0	52.0
49	56.7	64.0
61	0.0	
66	0.0	
73	0.0	63.0
100	0.0	61.7

Table 9: Effect of Xanthan Gum addition on physical stability of multiple emulsion composition.

		Composition %(w/w)
W_1	H_2O	18.78
	NaCl	0.72
Oil	Octyl palmitate	10.02
	Abil EM 90	0.48
W_2	H_2O	54.9
	Betaine	9.7
	SDS	3.5
	Xanthan gum	0.4

Table 10: Stable formulation with octyl palmitate

		Composition %(w/w)	
W_1	H_2O	18.78	18.78
	NaCl	0.72	0.72
Oil	Light mineral oil	10.02	10.02
	Abil EM 90	0.48	0.48
W_2	H_2O	54.8	54.9
	Betaine	8.6	10.9
	SDS	6.2	3.9
	Xanthan gum	0.4	0.4

Table 11: Stable formulations Betaine/SDS

Experience	Formulation	Observation
1	Betaine alone	large droplets-double emulsion separation
2	SLES alone	medium /large droplets-double emulsion separation
3	Betaine+ Xgum	medium droplets-no separation
4	SLES+Xgum	low viscosity- double emulsion -separation
5	SDS + carbopol	high viscosity- single emulsion
6	Betaine + Carbopol	Large droplets-double emulsion separation
7	Betaine + SLES	form initial gel-single emulsion
8	#3 then SLES	double emulsion-no separation

Table 12: Observation from a series of experiment based on the same basic formulation and mechanical stirring.

Run	Eff. Diam. (nm)	Half Width (nm)	Polydispersity
1	348.0	99.0	0.159
2	380.0	159.1	0.321
3	240.2	83.7	0.121
4	302.3	157.9	0.273
5	340.4	187.7	0.304
Mean	282.3	137.5	0.236
Std. Error	18.4	19.7	0.040
Combined	269.8	126.1	0.218

Table 13: Particle size determination using light scattering method

Radius (r) nm	γ (mN/m)	m(mol/m^3)	%NaCl
10	10	2.69	0.016
100	10	0.269	0.0016
200	10	0.134	0.0008
400	10	0.067	0.0004

Table 14: Estimating the minimum salt concentration required for various γ = 10mN/m and r to prevent Ostwald ripening in a water/oil emulsion

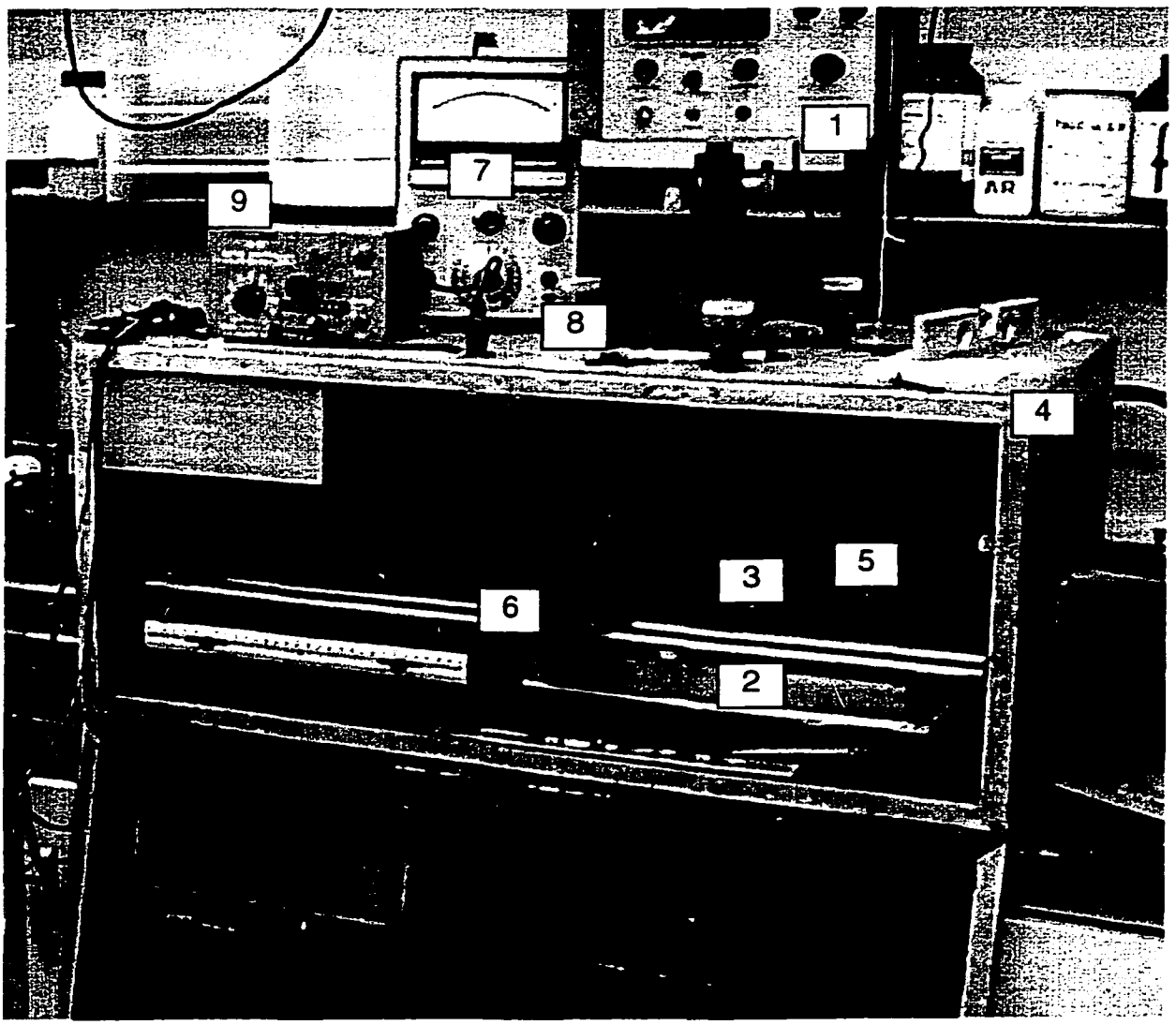

Figure 1: Experimental apparatus for measuring surface pressure and surface potential.

1.Transducer-amplifier	6.Mechanical drive
2.Fused silica trough	7.Potetiometer
3.Moving Teflon barrier	8.Alga micrometer syringe
4.Farraday Box	9.Speed control for mechanical drive
5.Support for Pt blade	

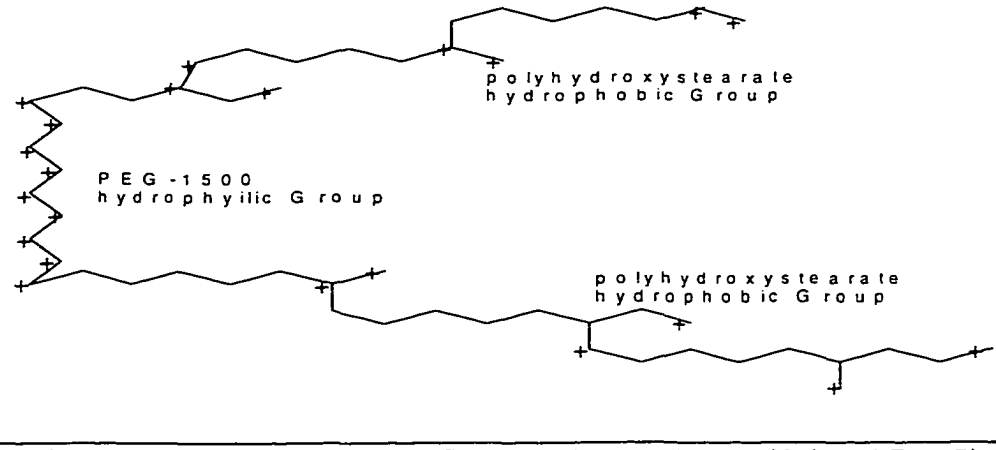

Schematic Structure of A-B-A block copolymer (Arlacel P135)

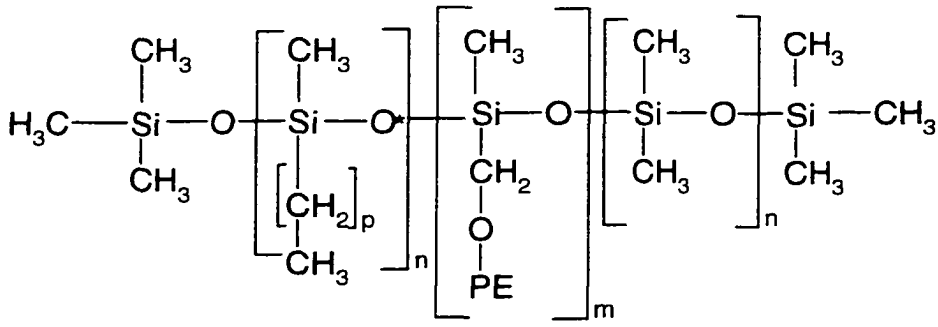

Cethyl dimethicone copolyol (Abil Em90)

2

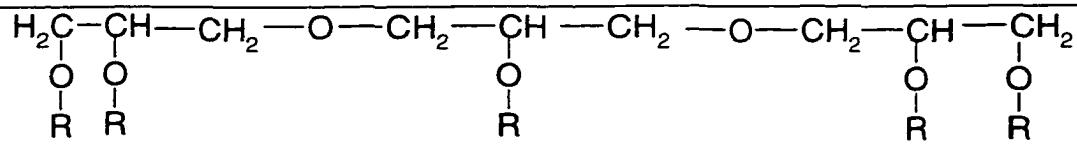

Polyglycerol esters of ricinoleic acid (PGR)

Figure 2: Structure of the surfactants that allow to prepare a stable W1/O/W2 emulsion over 1 month period at room temperature.

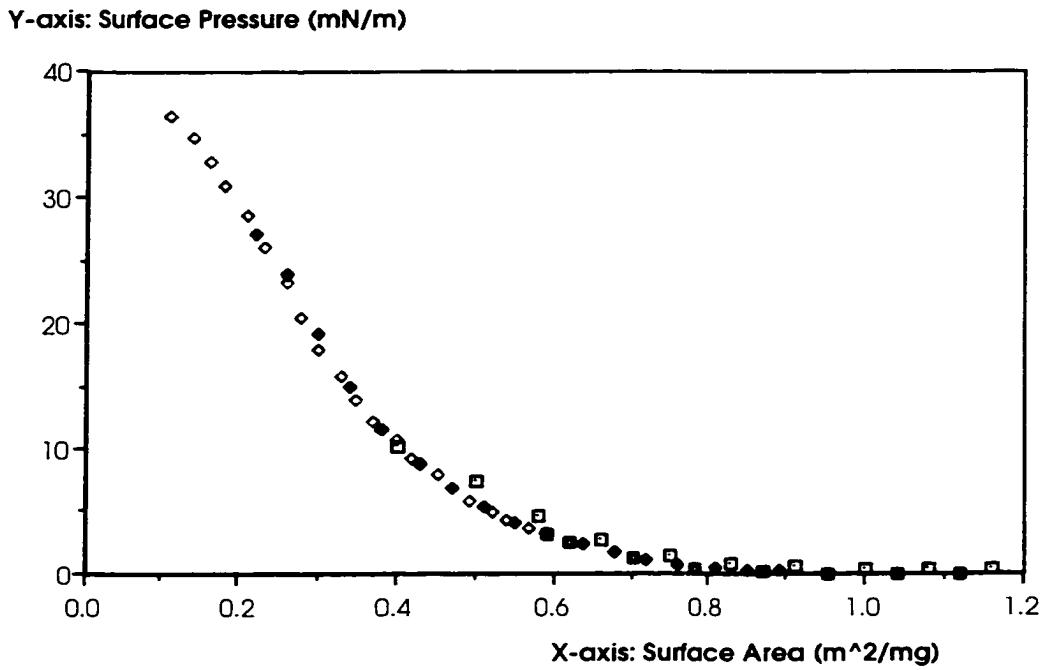

Figure 3: Compression - decompression isotherm of a film of cetyl dimethicone copolyol spread over a 1% NaCl solution.

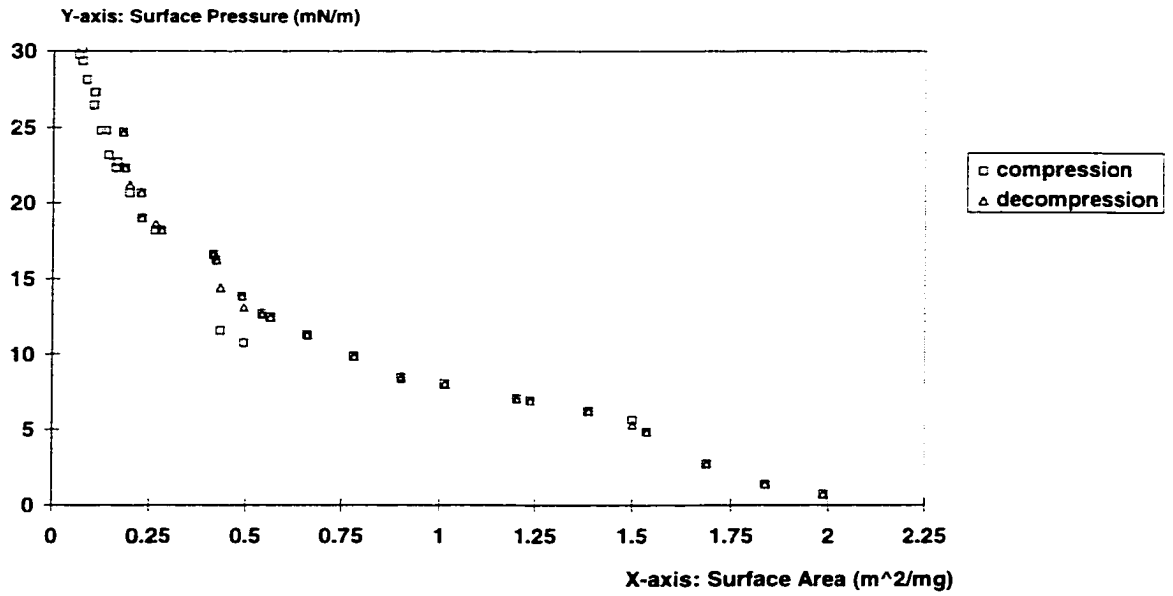

Figure 4: Compression - decompression isotherm of a film of polyglycerol ester of ricinoleic acid spread over a 0.1% KCl solution.

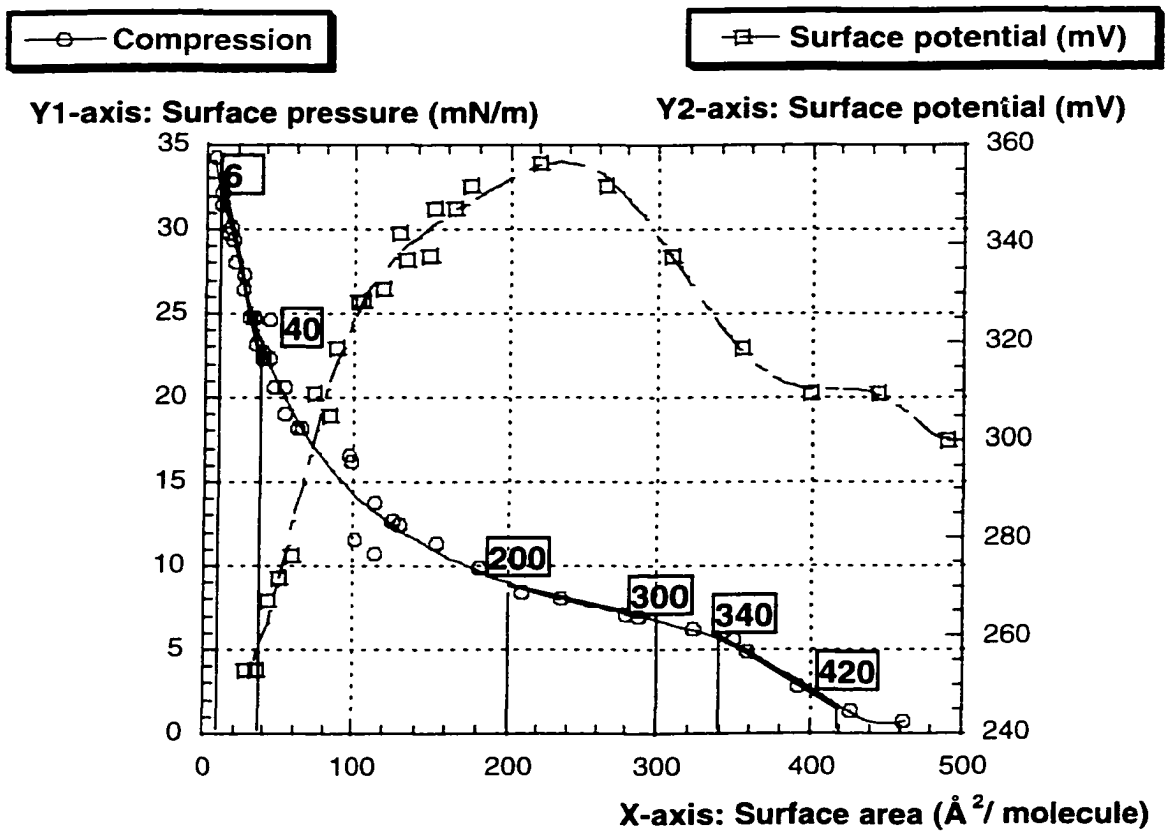

Figure 5: Surface pressure and surface potential of a film of polyglycerol ester of ricinoleic acid spread over a 0.1% KCl solution.

Segment Å^2 /molecule	π (mN/m)	Elasticity (m/N) at mid-range surface
420	2.05	*A*(mid-range): 380 Elasticity: 56.1
340	5.8	
300	6.80	*A*(mid-range): 250 Elasticity: 174
200	9.1	
40	23.0	*A*(mid-range): 23 Elasticity: 123
6	35.0	

Figure 6: Elasticity of a film of polyglycerol ester of ricinoleic acid at some critical surface area.

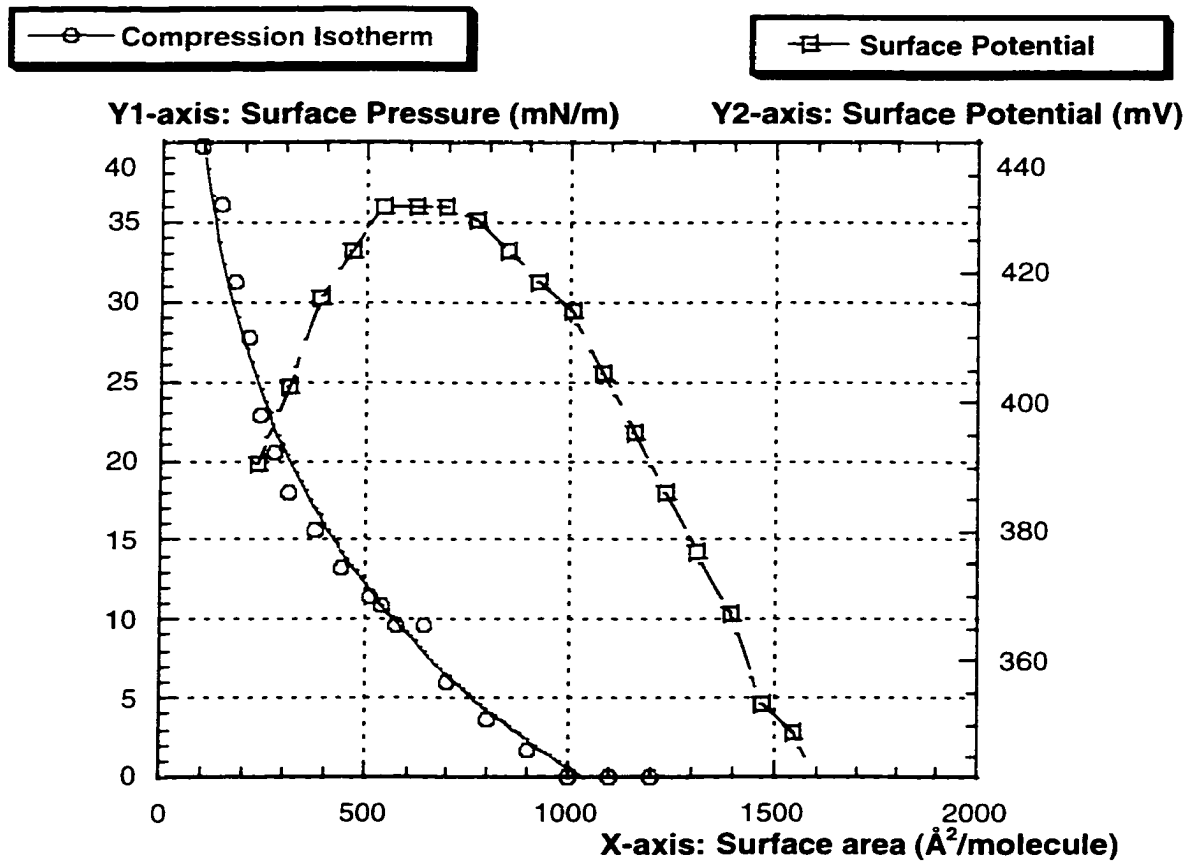

Figure 7: Surface potential of a film of PEG- polyhydroxystearate copolymer spread over a 0.1% KCl solution.

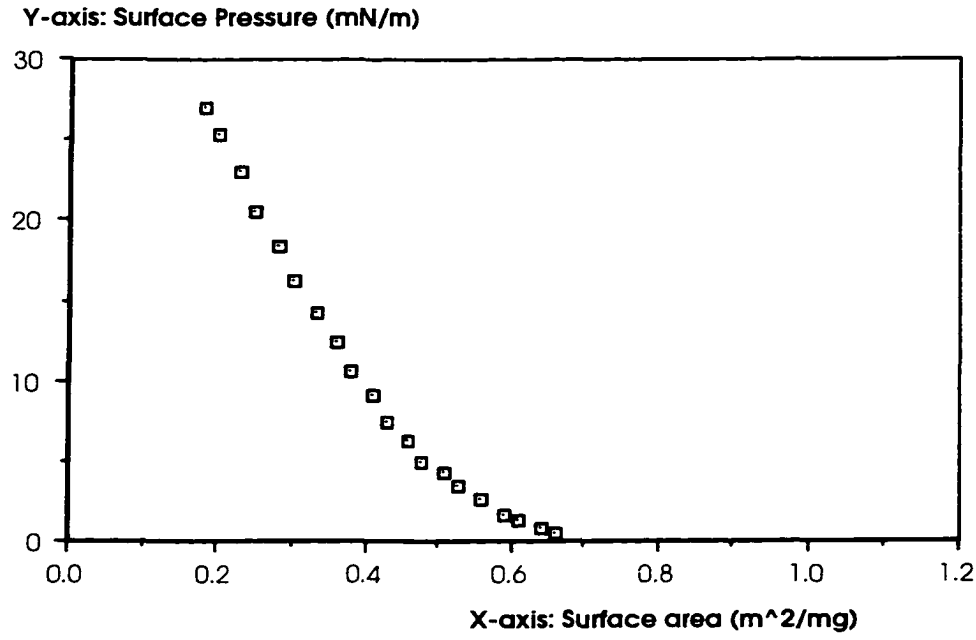

Figure 8: Compression isotherm of a duplex film Cetyl Dimethicone Copolyol/Hexadecane, spread over a 1% NaCl solution.

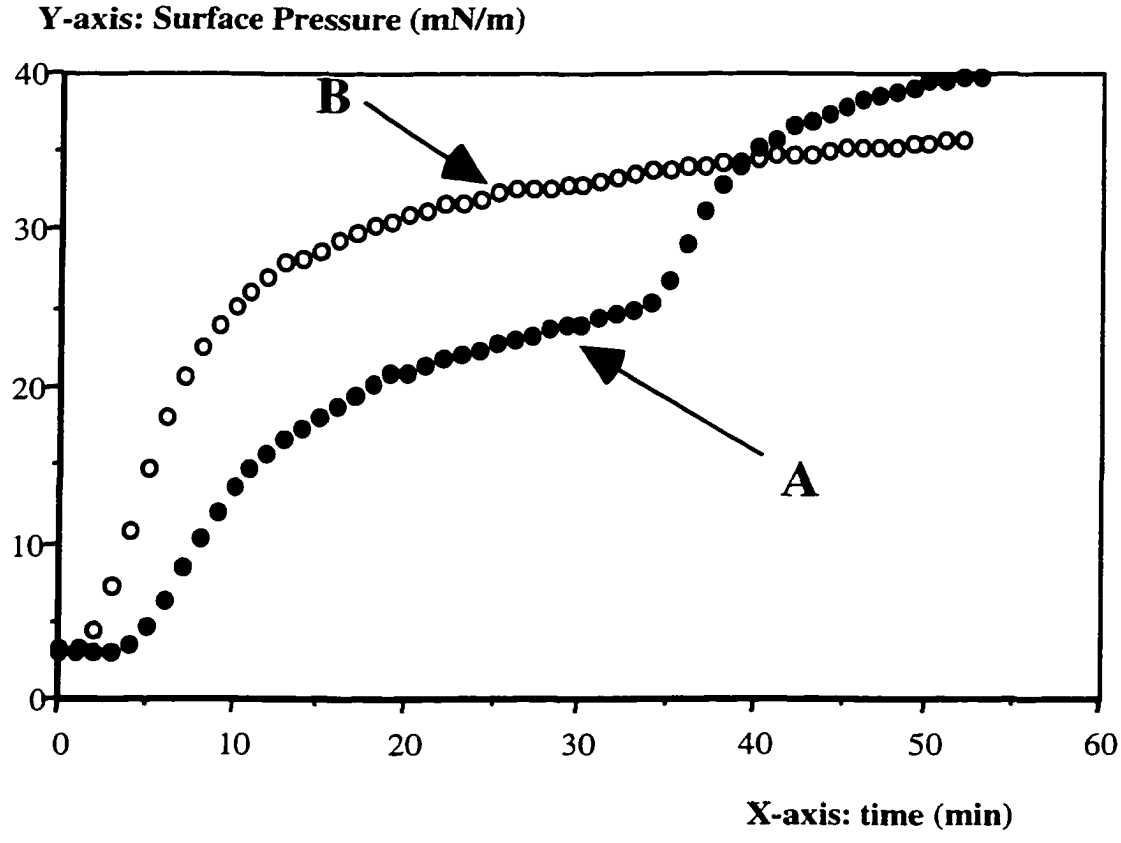

Figure 9: Evolution of the surface tension as a function of time after injection of 3 mg SLES and/or Betaine under a cetyl dimethicone film compressed at 3 mN/m. Curve A: injection of Betaine Followed by injection of SLES. Curve B: injection of SLES followed by injection of Betaine.

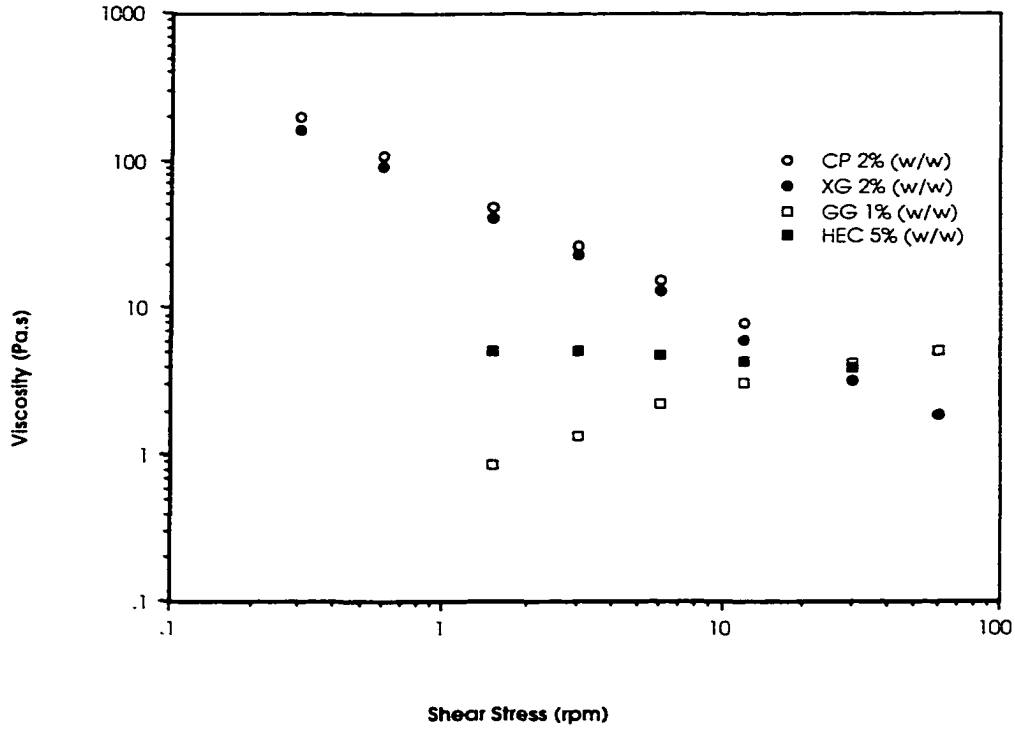

Figure 10: Viscosity as a function of shear stress for various polymers (xanthan gum (XG), hydroxyethylcellulose (HEC), guar gum (GG), carbopol 941 (CP)). Solutions prepared in water.

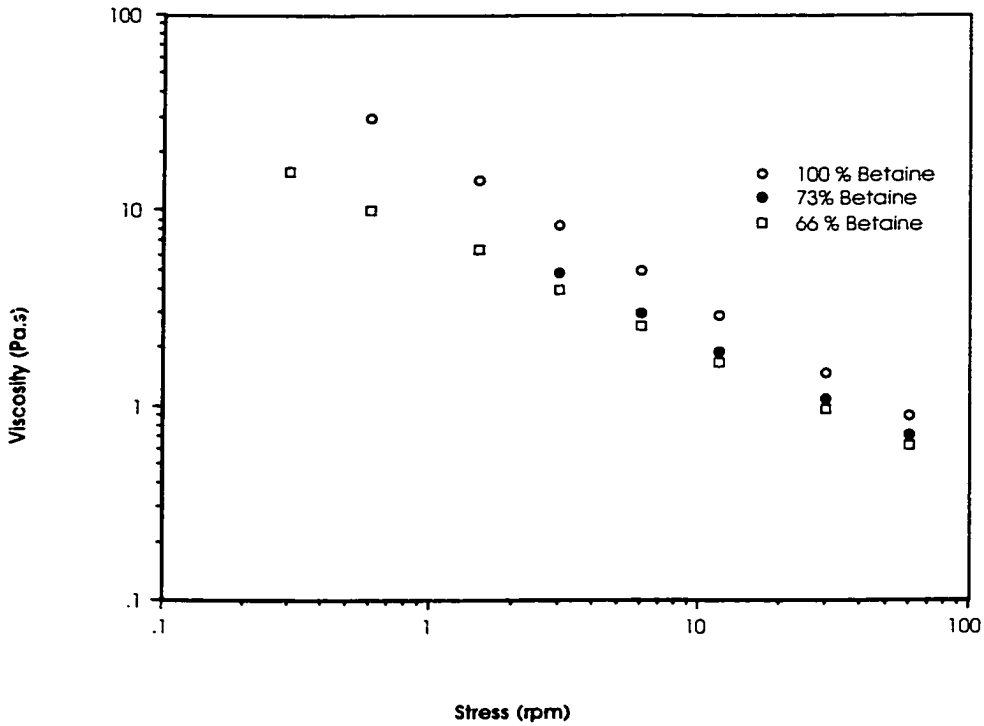

Figure 11: Viscosity as a function of shear stress for the stable formulations containing Betaine and Sles.

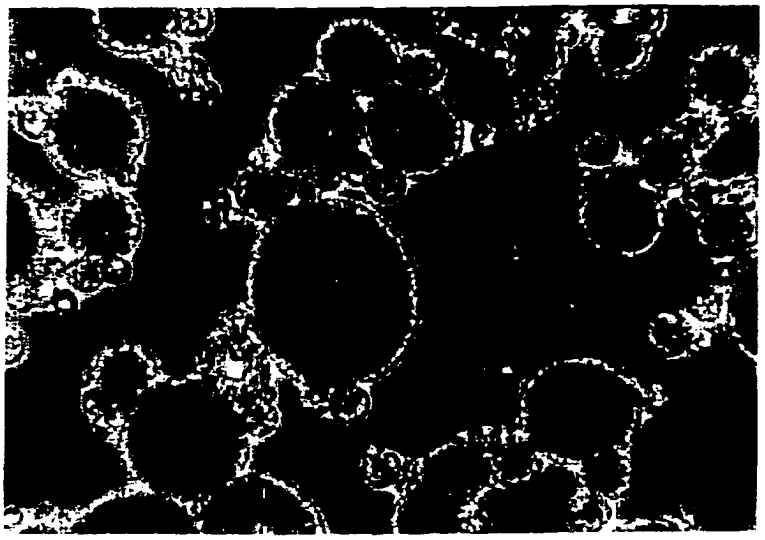

Figure 12: Picture taken after 1 day for the standard formulation with 32.3% (w/w) of Tego Betaine F and 17.7% of Steol CS 330. Magnification x350, no dilution, room temperature.

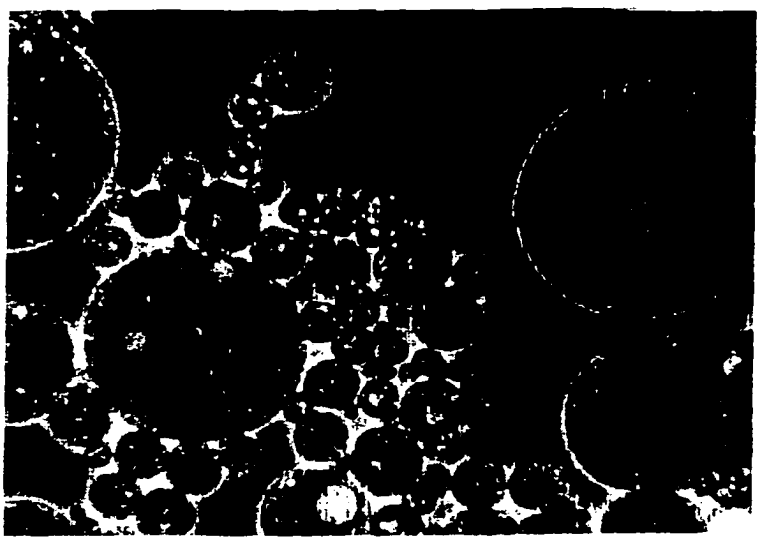

Figure 13: Picture taken after 220 days for the standard formulation with 32.3% (w/w) of Tego Betaine F and 17.7% of Steol CS 330. Magnification x350, no dilution, room temperature.

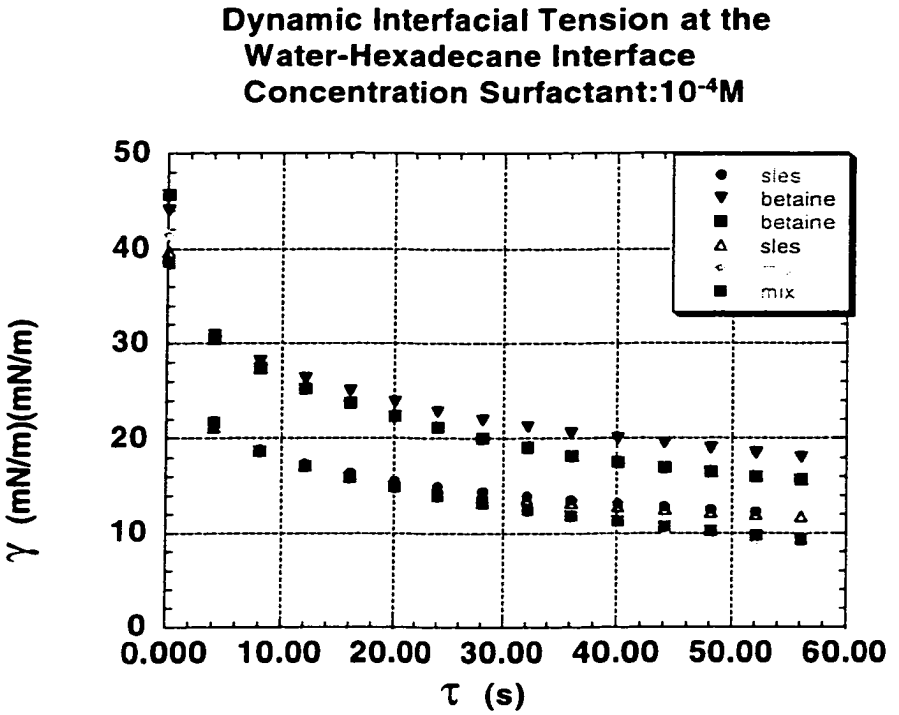

Figure 14: Surface tension relaxation function of time in clean interface (Hexadecane/Water) adsorption.

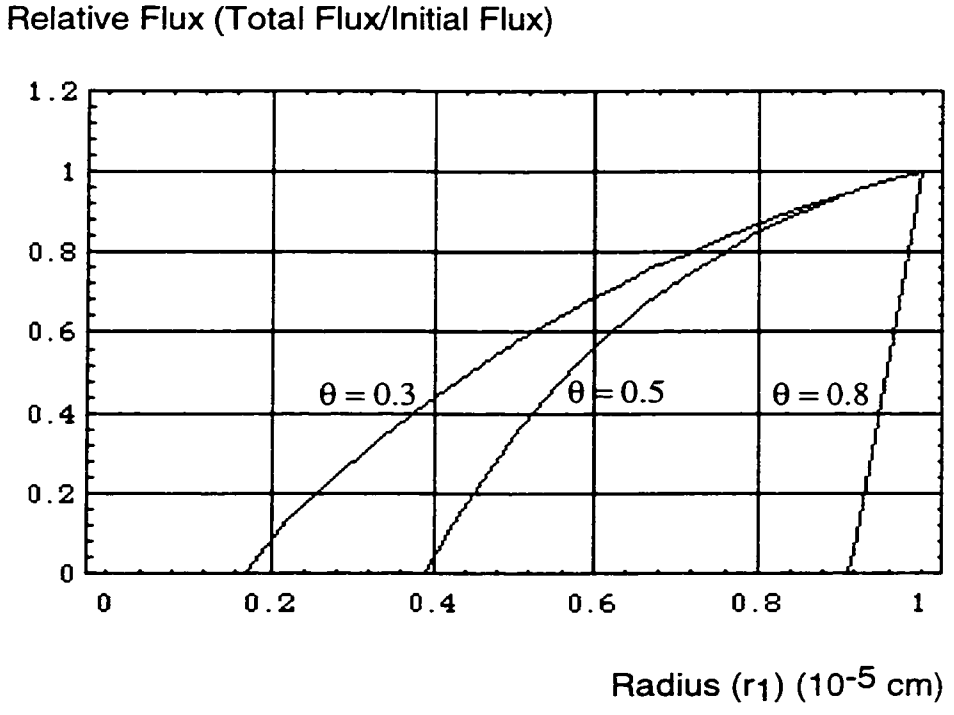

Figure 15:Evolution of the Relative Flux of water (Total Flux of water divided by the initial flux) versus the radius (r_1), for different initial radius ratios. K_o is taken equal to K_I

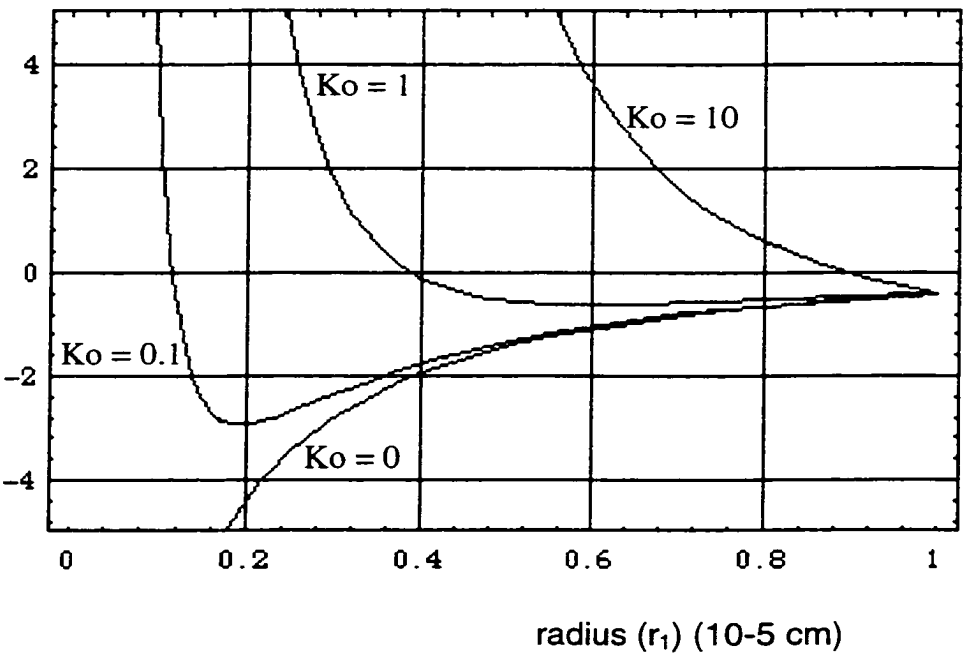

Figure 16: Evolution of the Relative flux of water (as in figure 1) versus the radius r_1, for different values of K_o, i.e. different concentrations of insoluble solute.

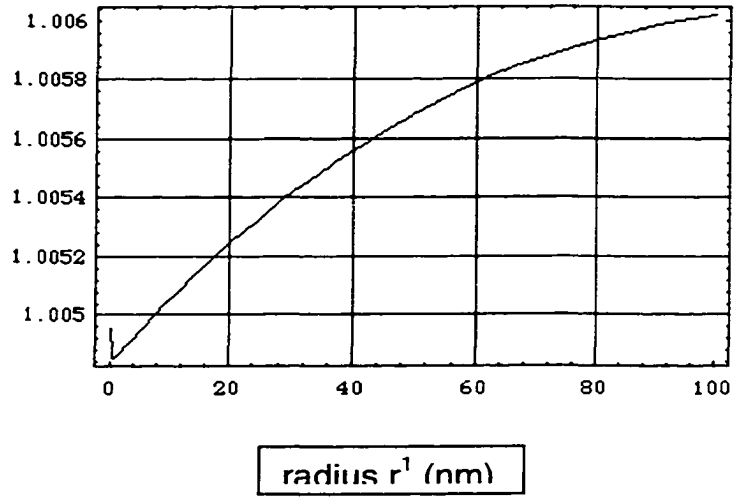

Figure 17 : Evolution of the mean concentration of the dispersed solvent in the continuous phase, with a diminution of the size of the smaller droplet.

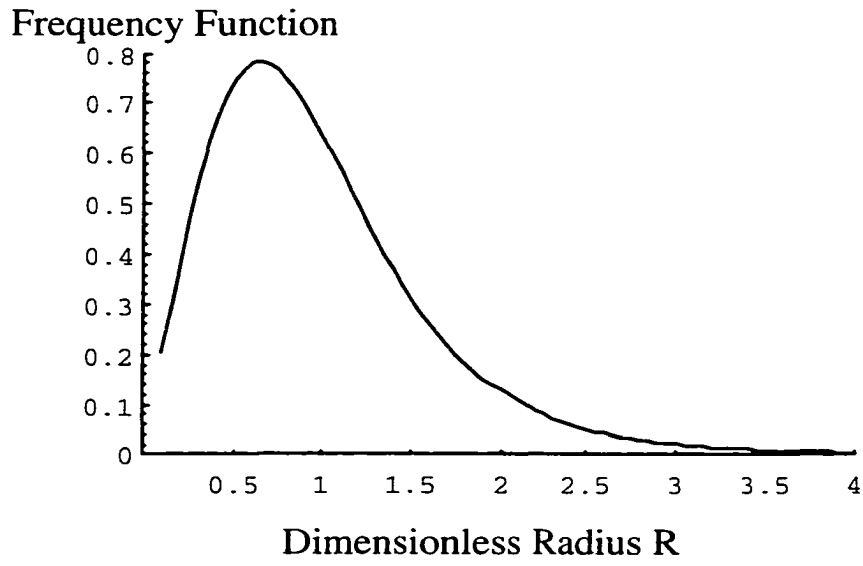

Figure 18: Distribution of de Vries.

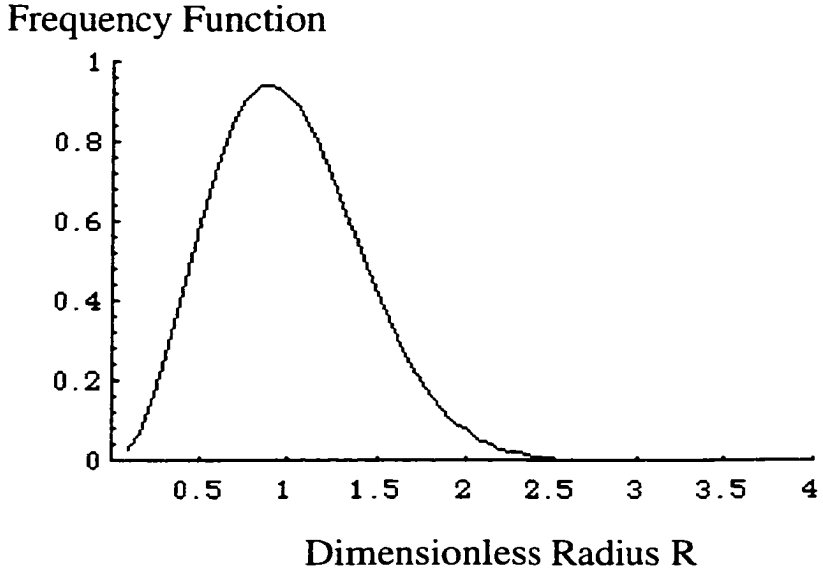

Figure 19: Distribution of Bayens.

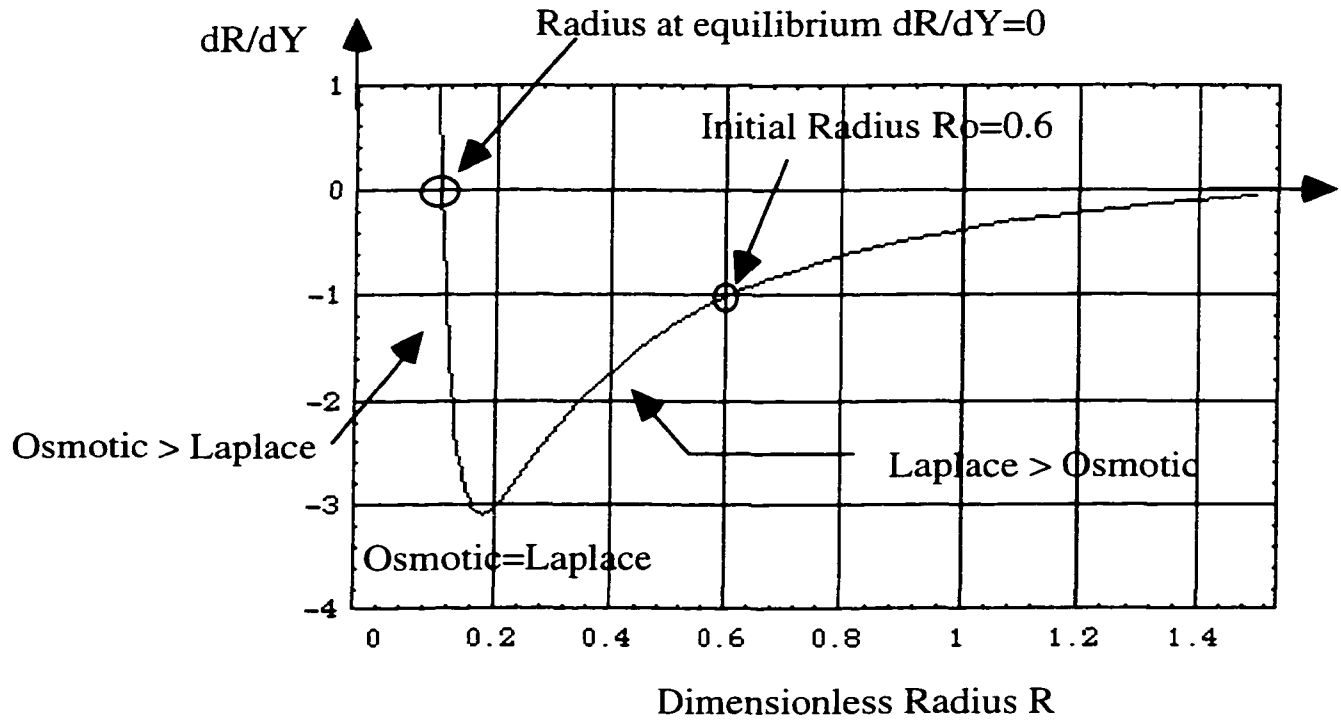

Figure 20: Plot of dR/dY as a function of the radius R for

Φ = 0.05, R_{21} = 1.5, R_o = 0.6

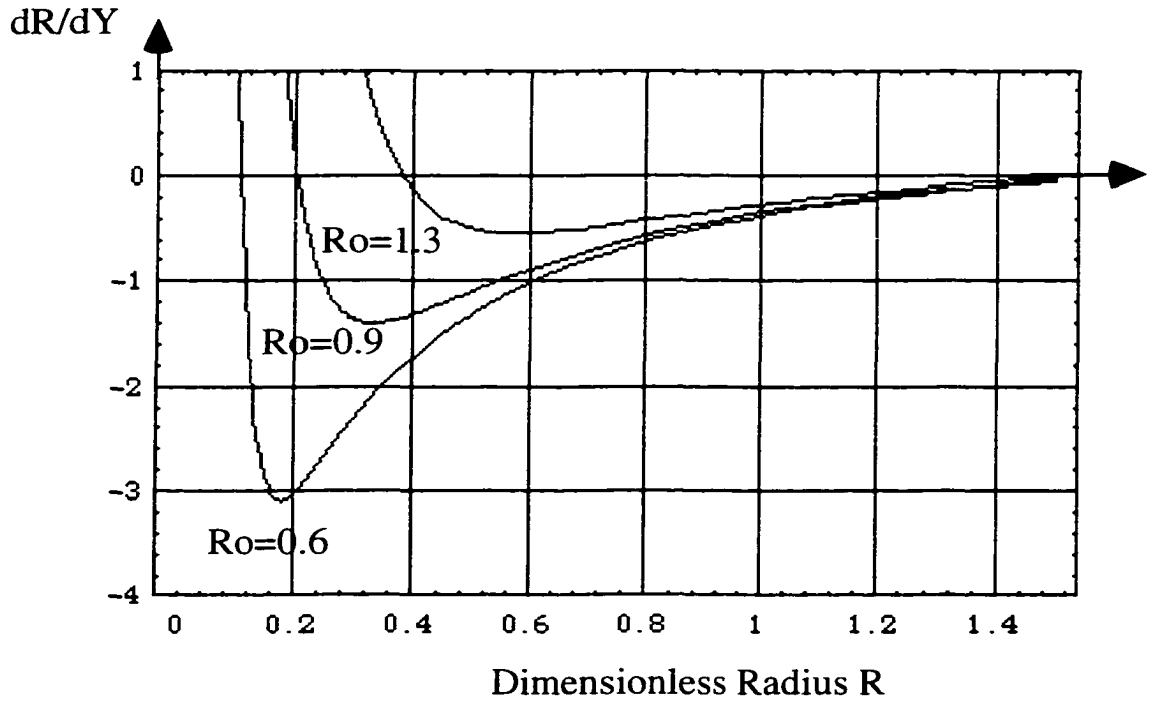

Figure 21: Plot of dr/dt for several initial radii (Ro) and with $\Phi = 0.05$, $R_{21} = 1.5$.

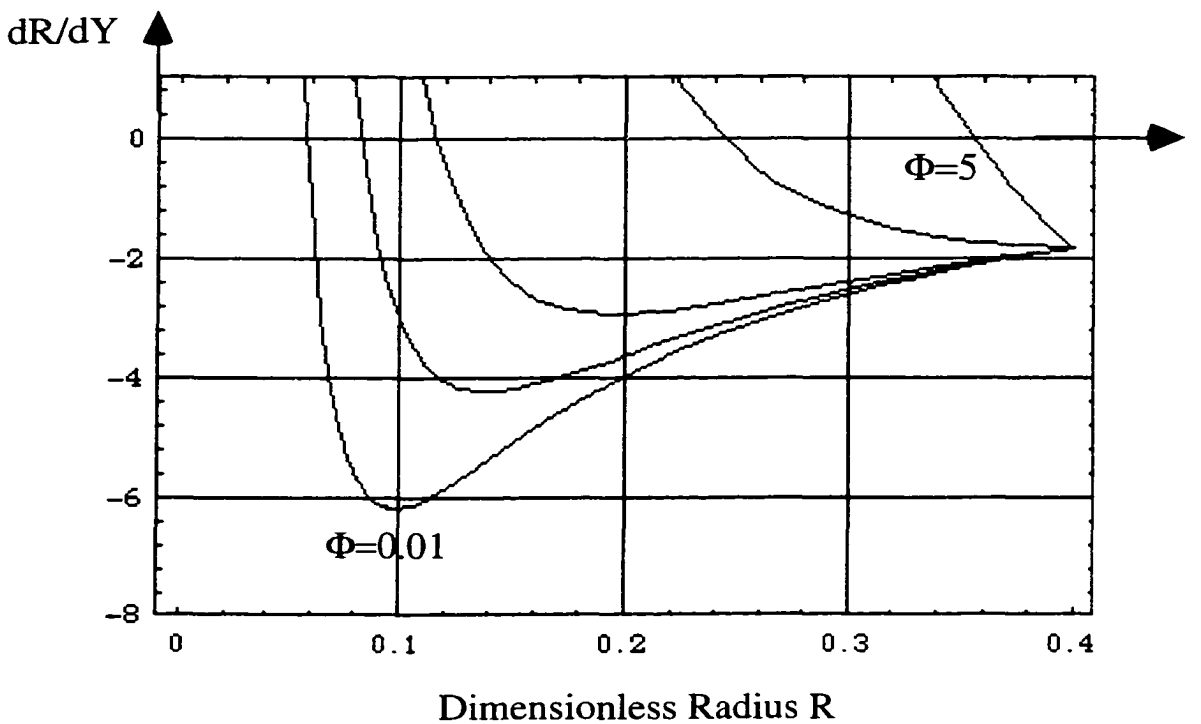

Figure 22: Effect of increasing the osmotic pressure

(Φ = 0.05, 0.1, 0.2, 1, 5) for R_{21} = 1.5

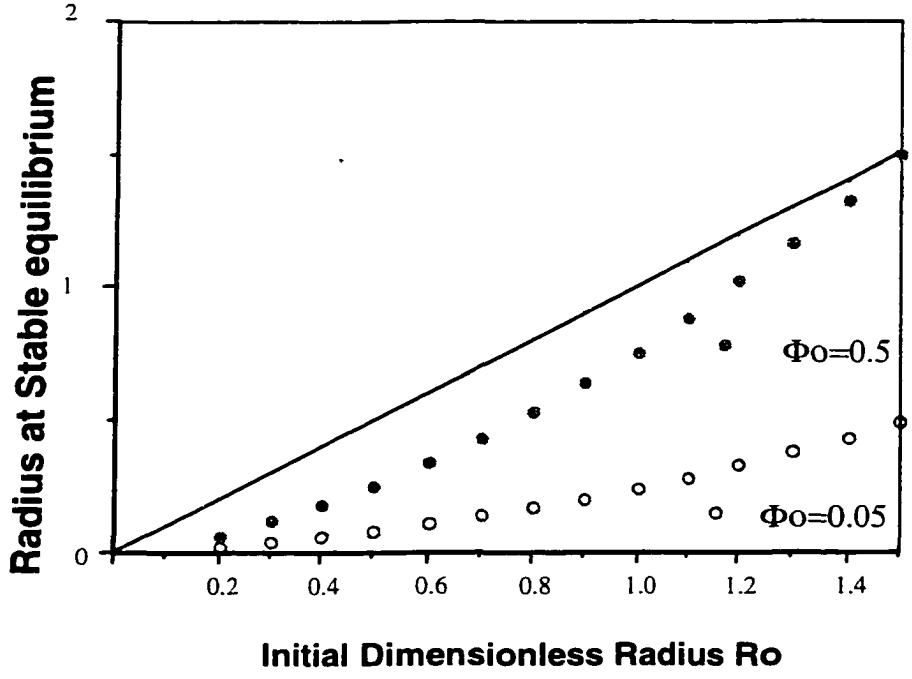

Figure 23: Radius at equilibrium versus Initial radius Ro

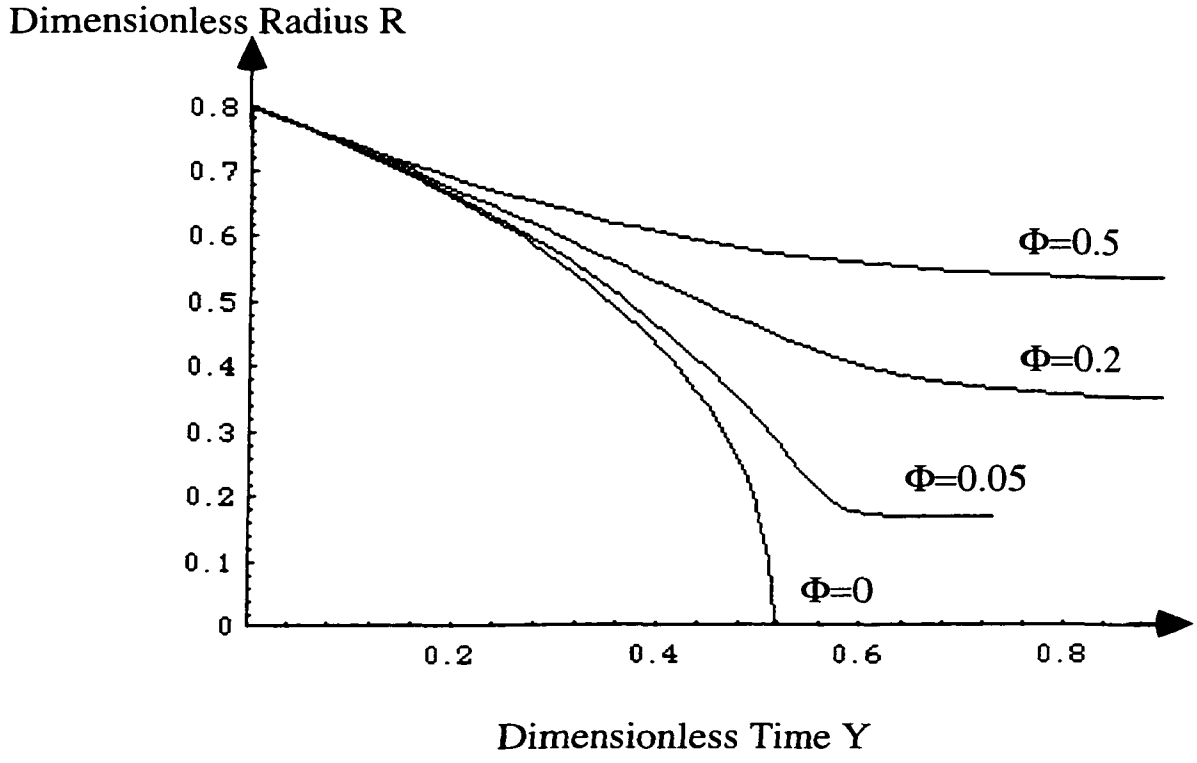

Figure 24: Curves of radius versus time for a bubble with and without an osmotic pressure, with R_o = 0.8, R_{21} = 1.5 and Φ = 0, 0.05, 0.2, 0.5.

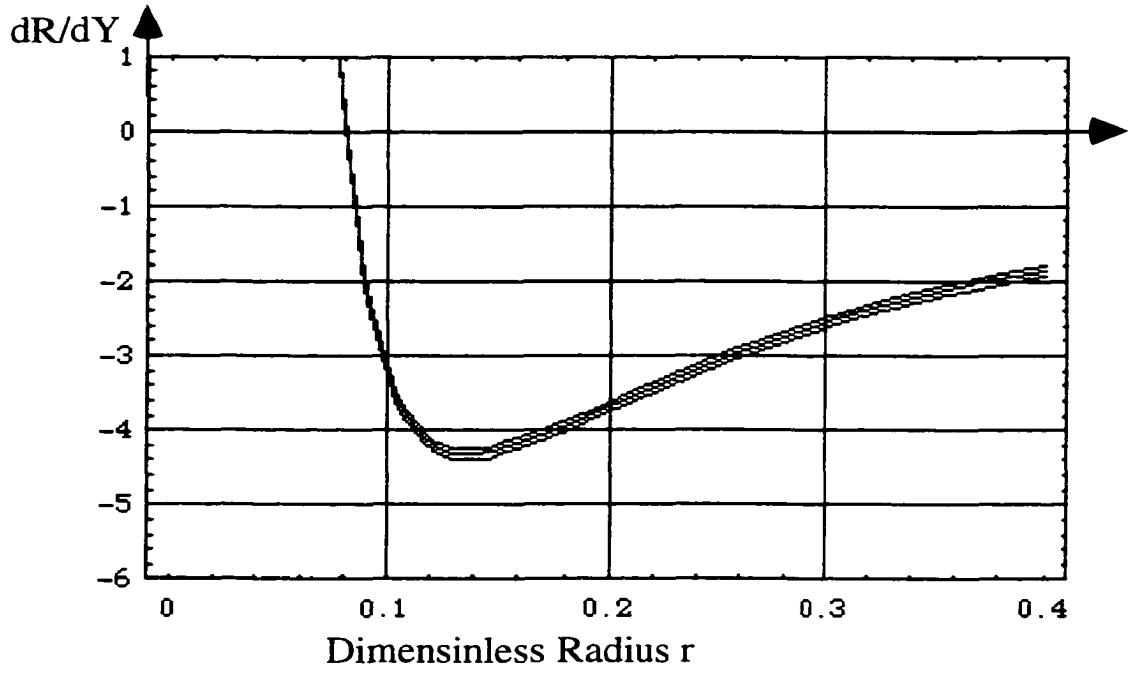

Figure 25: Plot of dR/dY for different R_{21} (1.5, 1.7, 2) and Φ = 0.05,

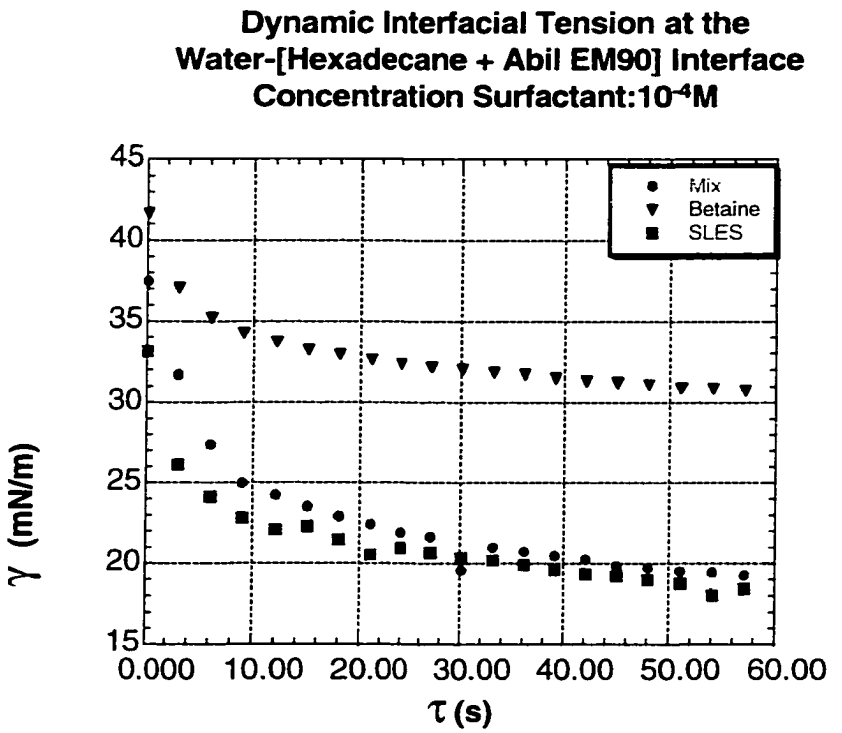

3

Figure 26: Surface tension relaxation function of time in clean surface (Hexadecane + Abil EM 90/Water) adsorption.

8 References

[1] J.L. Grossiord, M. Seiller and F. Puisieux, Rheol.Acta., 32 , **1993**, 168-180.

[2] M.L. Cole, T.L. Whateley, J. Controlled Release, 49 (1), **1997**, 51-58.

[3] C.H. Lee, J.S. Tsai, J.J. Huang, Shipin Kexue, 24(3), **1997**, 269.

[4] S. Nakhare, S.P. Vyas, J. Microenscapsulation, 12(4), **1995**, 409.

[5] H. Ohkouchi, M. Nakano, Drug Delivery Systems, 9(1), **1994**, 31.

[6] A. Silva Cunha, J.L. Grossiord, F. Puisseux, M. Seiller, J. Microencapsulation, 14 (3), **1997,** 311-319.

[7] C. Chen, Y. Tu and H. Chang, J. Agric. Food Chem, **1999,** *47*, 407-410

[8] Y. Yoo, S. Lim, Polilino, **1997,** *21(3)*, 490-498

[9] T. Kover, I. Csoka, I. Eros, Hung. Pharmazie, **1997**, *52(2)*, 166-167

[10] H.L Rosano, F. Gandolfo and J.P. Hidrot, Colloid Surf. A., **1998**, *138*, 109-121

[11] M.P. Aronson, M.F. Petko, J. Colloids Interface Sci., **1993**, *159*, 134

[12] M.F. Ficheux, L. Bonakdar, F. Leal-Calderon, J. Bibette, Langmuir, **1998**, *14*, 2702-2706

[13] B. Ute, Granum-Verlag, **1996**, *268*, 46-59

[14] H.L.Rosano, F.Gandolfo, and J. P. Hidrot, Colloid Surfaces A., 138, **1998**, 109.

[15] S. Magdassi, M. Frenkel, N. Garti, J. Dispersion Sci. and Technology, **1984**, 5, 49.

[16] N. Garti, Colloids Surf. A., **1997**, 123, 233.

[17] P. Hameyer and K.R. Jenni, 18th International I.F.S.C.C.-Congress, 3-6 October **1994**, Venice, Italy.

[18] ICI publication, 42-8E/3966.2Ed.S.DH/April **1997**.

[19] N. Garti, Colloids Surf. A., **1997**, *123*, 233

[20] Ibid., Chap. 4- 5.

[24] H.L Rosano, S. Habif, C. Oleksiak, Surfactant in Solution, **1991**, *11*, 431-56

[25] S. Habif, P. E. Normand, C. B. Oleksiak, H. L. Rosano, Biotechnol. Prog., **1992**, *8*, 454-457

[26] H.L.Rosano, S. Habif, C. Oleksiak, J.L.Cavallo and T.J.Pelura, Surfactants in Solution, **1991**, 11, 125.

[27] H.L.Rosano, J. Soc. Cosmet. Chem., **1974**, 25, 609-619.

[28] Rajinder Pal, Encyclopedia. of Emulsion Tech., **1996**, 4, 112-118.

[29] P. Stroeve and P.P. Varanasi, J. Colloid Interface Sci., **1984**, 99(2), 360-373.

[30] J.L. Grossiord, M. Seiller, Les Cahiers de Rhéologie, **1997,** 15.

[31] E.H. Lucassen-Reynders, Encyclo. of emulsion tech., 4, **1996**, 63.

[32] H. P Grace, Chem.Eng. Sci., **1982,** 48, 277.

[33] R. A. de Bruijin, Chem. Eng. Sci., 48, **1993**, 2877.

[34] F.D.Rumscheidt , S.G. Mason, J. Colloid Sci., 16, **1961,** 238.

[35] J. Buno , L.T Lee and B. Cabane, Langmuir, **1999**, 15, 22, 7585-7590.

[36] W. L. P. Kyziztos, Langmir, **2000**, *16*, 7612-7617.

[37] A. S. Kabalnov and E. D. Shchukin, Colloid and Interface Sci., **1992,** 38, 69-97.

[38] H.M.Princen and S.G. Mason, Colloid Sci., 20, **1965**, 353-375.

[39] P.Lemlich, Ind. Eng. Chem. Fundam., 17, 2, **1978**, 89-93.

[40] P. Walstra, "Encyclopedia of Emulsion Technology, Vol. 4" (P. Becher, Ed.), **1996**, 1-62.

[41] A. Monsalve and R. S. Schechter, Colloid Interface Sci. **1984**, 97, 2, 327.